

https://dspace.org/

Design and Validation of an Arterial Pulse Wave Analysis Device

Salter, Geoffrey Douglas

2006-11-17T07:27:27Z
http://hdl.handle.net/10539/1824

Downloaded from a DSpace repository. https://dspace.org/

Design and Validation of an Arterial Pulse Wave Analysis Device

Geoffrey Douglas Salter

A dissertation submitted to the Faculty of Engineering and the Built Environment, University of the Witwatersrand, Johannesburg, in fulfilment of the requirements for the degree of Master of Science in Engineering.

Johannesburg, May 2005

Declaration

I declare that this dissertation is my own, unaided work, except where otherwise acknowledged. It is being submitted for the Degree of Master of Science in Engineering in the University of the Witwatersrand, Johannesburg. It has not been submitted before for any degree or examination in any other university.

Signed this __ day of _____ 20__

_____

Geoffrey Douglas Salter.

Abstract

Arterial pulse wave analysis studies the wave shape of the blood pressure pulse. The pulse wave provides more information than the extreme systolic and diastolic pressures, measured with a cuff sphygmomanometer. The aim of the research is to investigate the design issues in a pulse wave analysis system, and to compare these to a commercially available system. The system was compared and validated by measuring the pulse wave at the radial artery (wrist) using the non-invasive technique of arterial tonometry. The design conformed to the IEC-601 safety standard to ensure patient safety. The data was compared against the data from the commercial system and analysis was performed in the time and frequency domain. The performance of the design suggests that, in some respects, the design was comparable to the commercial system, however, a number of performance characteristics fell short of the commercial system. Suggestions have been made to address these problems in further research.

Acknowledgements

The financial assistance of the Department of Labour (DoL) towards this research is hereby acknowledged. Opinions expressed and conclusions arrived at, are those of the author and are not necessarily to be attributed to the DoL.

Professor F. Raal whose initial discussion and funding led to this project.

Professor Gavin Norton for allowing me to make use of the facilities at the Medical School, University of the Witwatersrand.

Dr David Rubin and Dr Charles Pritchard for their guidance, advice and assistance throughout this research,

Peter Spyres for his assistance in the design of the Electrocardiogram and for his generous donation of ECG electrodes for this research,

John Buyers and Brittan Health-Care for testing the device for compliance to IEC–601 standards for electrical safety,

Simon Hoffe for his assistance with the data acquisition equipment and software,

Nomonde Molebatsi for her expert assistance at Wits Medical School during the testing stages.

Contents

Declaration **1**

Abstract **2**

Acknowledgements **3**

Contents **4**

List of Figures **9**

List of Tables **12**

List of Abbreviations **14**

1 Introduction **16**

1.1 Introduction 16

1.2 Problem Statement 17

1.3 Research Methods 18

1.4 Specifications and Limitations 18

1.5 Structure of Report 19

2 Background of Pulse Wave Analysis 21

2.1 Overview 21

2.2 Description of Pulse Wave Shape 22

2.2.1 Wave Reflection 24

2.2.2 Augmentation Index 25

2.2.3 Aortic Pulse Estimation 25

2.3 Electrocardiogram 27

2.4 Measurement Techniques 28

2.4.1 Arterial Tonometry 29

2.4.2 Photoplethysmography 30

2.4.3 Doppler Ultrasound 30

2.4.4 Other Methods 30

2.5 Factors Affecting Pulse Wave Shape 31

2.5.1 Physiological Factors 31

2.5.2 Arterial Diseases 32

2.6 Summary 33

3 Hardware 34

3.1 Overview 34

3.2 Design Overview 35

3.2.1 Arterial Tonometry Design 35
3.2.2 Electrocardiogram Design 36
3.2.3 Assembly 38
3.3 Signal Detection 38
3.4 Amplification 40
3.4.1 Pulse Amplification 40
3.4.2 ECG Amplification 41
3.5 Noise Reduction 42
3.6 Patient Safety and Isolation 45
3.6.1 Electrical Isolation 45
3.7 Testing and Calibration 46
3.7.1 Electrical Safety Compliance Test 46
3.7.2 Sensor Calibration 47
3.8 Data Acquisition 48

4 Testing and Data Analysis Methods 50

4.1 Overview 50
4.2 Measurement Procedure 50
4.2.1 Ethics Approval 52
4.3 Data Preparation 53
4.3.1 Signal Enhancement 53

4.3.2 Pulse Wave Calibration 54

4.4 Pulse Foot Identification 55

4.5 Performance Analysis 59

4.5.1 Pulse Wave Quality 59

4.5.2 Sphygmocor Comparison 62

4.5.3 Frequency Analysis 64

5 Test Results **67**

5.1 Overview 67

5.2 Comparison of Testing Procedures 67

5.3 Results of Pulse Foot Identification 69

5.4 Quality of Pulse Wave Shape 70

5.5 Comparisons Against Sphygmocor 73

5.6 Frequency Analysis 76

5.6.1 Frequency Spectrum 76

5.6.2 Impulse Response 77

6 Conclusion **79**

6.1 Discussion 79

6.2 Further Research 81

6.3 Conclusion 83

A Pulse Wave Analysis History **85**

B Hardware Circuits Description **87**

B.1 Pressure Sensor Circuit 87

B.2 Amplification Circuits 88

B.2.1 Pressure Amplification 88

B.2.2 ECG Amplification Circuit 90

B.3 Filter Circuits 91

B.4 Isolation Circuit 92

B.5 Circuit Diagrams 94

C Measured Data and Results **96**

C.1 Recorded Data 96

C.2 Results of Pulse Foot Calculation 101

C.3 Results of Time Analysis 103

C.4 Frequency Spectrum Results 107

D IEC Test Results **112**

E Ethics Approval **116**

References **118**

List of Figures

2.1 Example of pulse wave shape 22

2.2 Radial to aortic estimation 26

2.3 An electrocardiograph illustrating the QRS complex 27

3.1 Block diagram of arterial tonometry system 36

3.2 Block diagram of ECG amplifier 37

3.3 Comparison of the different sensors 39

3.4 ECG trace without a notch filter 44

3.5 ECG trace with a notch filter 44

3.6 Calibration curve of system 48

4.1 Location of pressure transducers on the wrist 52

4.2 Ten second recording of pulse measured from both systems . . . 53

4.3 The individual pulse periods calibrated with respect to the average pulse 54

4.4 Time variation of Systolic peak 57

4.5 Example of recorded data 60

4.6 Parameters for comparison of the wave shapes 64

4.7 Example of comparison of the frequency spectrum 65

4.8 Impulse response of the designed system. 66

5.1 Comparison of pulse quality 69

5.2 Results from the different methods of calculating the foot of the pulse 71

5.3 Results of quality assessment 72

5.4 Results of comparison measurements 74

5.5 Comparison of the pulse between the two systems 76

5.6 Magnified section of the frequency spectrum 77

5.7 Transfer function of the designed system 78

B.1 Excitation circuit for the pressure sensor 88

B.2 Sensor amplification circuit 89

B.3 ECG amplifier and right leg drive circuit 90

B.4 Fourth order Butterworth filter used for signal conditioning . . . 91

B.5 First order bandpass filter 91

B.6 Twin-T notch filter circuit diagram 92

B.7 Isolation circuit using an optocoupler 93

B.8 Schematic of main circuit board 94

B.9 Schematic of sensor unit circuit 95

C.1 Measured results of subject 1 97

C.2 Measured results of subject 3 97

C.3 Measured results of subject 4 98

C.4 Measured results of subject 5 98

C.5 Measured results of subject 6 99

C.6 Measured results of subject 7 99

C.7 Measured results of subject 8 100

C.8 Measured results of subject 9 100

C.9 Frequency spectrum of subject 1 107

C.10 Frequency spectrum of subject 3 108

C.11 Frequency spectrum of subject 4 108

C.12 Frequency spectrum of subject 5 109

C.13 Frequency spectrum of subject 6 109

C.14 Frequency spectrum of subject 7 110

C.15 Frequency spectrum of subject 8 110

C.16 Frequency spectrum of subject 9 111

List of Tables

3.1 Einthoven's 3-Lead ECG configuration 37

3.2 Tested opto-isolation amplifiers 46

4.1 Subject characteristics and clinical results 51

5.1 Results of methods to identify the foot of the pulse 70

5.2 Assessment of quality of pulse wave recording 71

5.3 Results of Sphygmocor comparison 75

C.1 Comparison of correlation coefficient. 101

C.2 Comparison of time variation of the systolic peak. 102

C.3 Comparison of RMS error between individual pulses. 102

C.4 Comparison of systolic pressure measured from designed system 103

C.5 Comparison of systolic pressure measured from sphygmocor system 103

C.6 Comparison of rise time of the systolic peak 104

C.7 Comparison of time to the dicrotic notch 104

C.8 Comparison of dicrotic notch value 105

C.9 Comparison of second systolic peak 105

C.10 Comparison of time to second systolic peak 105

C.11 Comparison of Root-Mean-Square (RMS) errors 106

List of Abbreviations

AiX	Augmentation Index
CC	Correlation Coefficient
CMRR	Common Mode Rejection Ratio
CRF	Chronic Renal Failure
CTR	Current Transfer Ratio
DAQ	Data Acquisition System
DBP	Diastolic Blood Pressure
DC	Direct Current
DFT	Discreet Fourier Transform
DSP	Digital Signal Processor
ECG	Electrocardiogram
FFT	Fast Fourier Transform
HPF	High-Pass Filter
IIR	Infinite Impulse Response
IMRR	Isolation Mode Rejection Ratio

LA	Left Arm
LPF	Low-Pass Filter
MAP	Mean Arterial Pressure
PSD	Power Spectral Density
PWA	Pulse Wave Analysis
PWV	Pulse Wave Velocity
RA	Right Arm
RMS	Root Mean Square
SBP	Systolic Blood Pressure
SD	Standard Deviation
USB	Universal Serial Bus

Chapter 1

Introduction

1.1 Introduction

Pulse wave analysis (PWA) is the study of the waveform of the blood pressure pulse. The arterial pulse is the most fundamental sign in clinical medicine and has been studied for over 100 years [1]. Traditional blood pressure measurements are recorded using a cuff sphygmomanometer, which only measures the extremes of the brachial artery pressure; i.e. the systolic and diastolic values [1]. Much more information can be retrieved by analysing the full time-dependent pulse wave shape. This allows physicians to give an improved diagnosis of cardiovascular diseases.

The pulse pressure can be measured internally (invasive) or externally (non-invasive). This research is based on non-invasive measurements. By focusing on the non-invasive measurements, readings can be acquired easily and with little medical knowledge. There are various techniques for non-invasive measurements of the pulse wave shape. These include arterial tonometry, Doppler ultrasound and photoplethysmography and are explained in Section 2.4. The method used for this research is arterial tonometry.

1.2 Problem Statement

Pulse wave analysis is an expanding field of research which has developed rapidly over the last decade. There have been many papers written about PWA which approach the topic with different objectives. The first approach is to study the wave shape using a particular measuring technique, normally tonometric methods, and relate PWA to arterial diseases. The second approach is to measure the pulse contour using a number of measuring techniques and to compare the validity of these techniques.

In the studies that compared measuring techniques, comparisons have been made between two or more different techniques. Mustafa and Feneley [2] and van Lieshout et al [3] have compared Doppler and photoplethysmography, Oliver and Webb [4] have compared photoplethysmography and arterial tonometry, and Brinton et al [5] have compared oscillometric methods with intra-arterial catheter recordings.

In disease related research, the pulse was measured using only one method. Cruickshank et al [6] used Doppler ultrasound and Hlimonenko et al [7] studied PWA using photoplethysmography. The majority of studies [8, 9, 10, 11, 12, 13, 14, 15, 16] have used arterial tonometry. Amongst these studies only Asmar et al [16] used a different pressure transducer (TY-306, Fukuda Co). The rest all used the Sphygmocor system (Atcor Medical, Australia), which incorporates the SPT-301 micromanometer by Millar Instruments.

The problem is that there have been few studies where different arterial tonometry systems have been compared against each other. Most researchers use the Sphygmocor system because it is commercially available and is easy to use. This has led to Sphygmocor dominating the arterial tonometry sector. There are other arterial tonometry systems such as the Colin CBM-7000, (ScanMed

Medical Instruments, UK) but these have been studied [17] and have been found unsuitable for intensive care use. The aim of the research is to investigate the design issues in a pulse wave analysis system, and to compare these to the Sphygmocor System.

1.3 Research Methods

The approach to the research consisted of two parts. The first was to build a device to measure the pulse wave shape. The system needed to be electrically safe to ensure patient safety. Arterial pulse signals have a small voltage range, so sufficient amplification and filtering was needed. Chapter 3 details the hardware design.

The second part of the research involved recording the pulse wave shape of different test subjects using the designed system and the commercial Sphygmocor system. The results from the designed system were compared and validated against the results from the Sphygmocor system.

Tests were conducted in the physiology labs at Wits Medical School. Ethics approval was required before any test on human subjects could commence. The device was electrically tested to ensure patient safety. The device must conform to IEC 601-1, which is the safety standard for medical equipment [18].

1.4 Specifications and Limitations

The designed system will be in direct contact with the patient's body while measuring the pulse and Electrocardiogram. The equipment will also be connected to a mains supply via the computer and data acquisition system (DAQ). It is therefore essential that the appropriate safety standards are maintained

to avoid the risk of electrical shock. For medical electrical equipment the standard is the **SABS IEC 60601-1 (or IEC 601-1) - Part1: General requirements for safety** [18].

According to this standard the device is classified as Class I type BF equipment. The relevant electrical specifications for such a device are defined as follows:

- The designed device is classed as INTERNALLY POWERED EQUIPMENT, however, because of its connection with the DAQ and computer it must comply to the requirements for Class I equipment.
- Class I equipment is required to have double or reinforced insulation. In the case where basic insulation is provided (such as a computer) a separate earth conductor is required.
- The patient auxiliary current and patient leakage current must not exceed 10μA under normal DC conditions and 50μA under a single fault condition.
- The earth leakage current must not be greater than 0.5mA under normal conditions.

The above specifications must be adhered to in order to maintain patient safety. The testing methods and results to ensure that these standards are met are presented in Section 3.7.

1.5 Structure of Report

The dissertation is split into several chapters. These include:

- **Pulse Wave Analysis Background:** This chapter explains the theory behind Pulse Wave Analysis (PWA), the benefits, and the previous studies of PWA. The purpose of the chapter is to give the reader a better understanding of PWA.

- **Hardware Design:** The majority of the work went into designing the device that was tested. This section describes the different sections of the circuit. The requirements for medical devices are presented. An explanation as to how these requirements are met in the design is given.

- **Testing and Analysis Procedure:** The device needed to be tested to determine its capabilities. This chapter consists of two parts: the first part explains the testing procedure. It includes the ethical requirements, hardware constraints and limitations of the test procedure. The second part explains the analysis of the results. This will explain what algorithms were applied to the results and why.

- **Test Results:** The results of the signal analysis are explained in this chapter. Possible explanations are given for the results, as well as possible conclusions. A discussion of the results is included.

- **Conclusion:** A discussion on the feasibility of developing a PWA system and the associated costs is presented

Chapter 2

Background of Pulse Wave Analysis

2.1 Overview

This chapter provides some insight into pulse wave analysis and its relation to arterial diseases. The shape of the arterial pulse wave is an augmentation of the forward traveling wave with the reflected wave. The amount of wave reflection is dependent on the arterial wall properties such as arterial stiffness and is expressed in terms of Augmentation Index. A mathematical transfer function has been used to estimate the waveform of the aortic artery for further assessment of arterial deseases. This approach has been studied extensively using various measuring techniques, all of which have respective advantages and disadvantages. The purpose of PWA can be seen in the section describing the medical conditions that affect the wave shape (Section 2.5). Although the medical relationships are not examined in this research, a discussion is included to assist the reader in understanding the purpose of pulse wave analysis. An explanation into the origins of pulse wave analysis is provided in Appendix A.

2.2 Description of Pulse Wave Shape

O'Rourke [19] describes the pulse wave shape as:

> "A sharp upstroke, straight rise to the first systolic peak, a definite sharp incisura, and near-exponential pressure decay in the late diastole."

This definition is explained further [20, 21]:
Arteries are compliant structures, which buffer the pressure change resulting from the pumping action of the heart. The arteries function by expanding and absorbing energy during systole (contraction of the cardiac muscle) and release this energy by recoiling during diastole (relaxation of the cardiac muscle). This function produces a smooth pulse wave comprising a sharp rise and gradual decay of the wave as seen in Figure 2.1. As the arteries age, they become less compliant and do not buffer the pressure change to the full extent. This results in an increase in systolic pressure and a decrease in diastolic pressure.

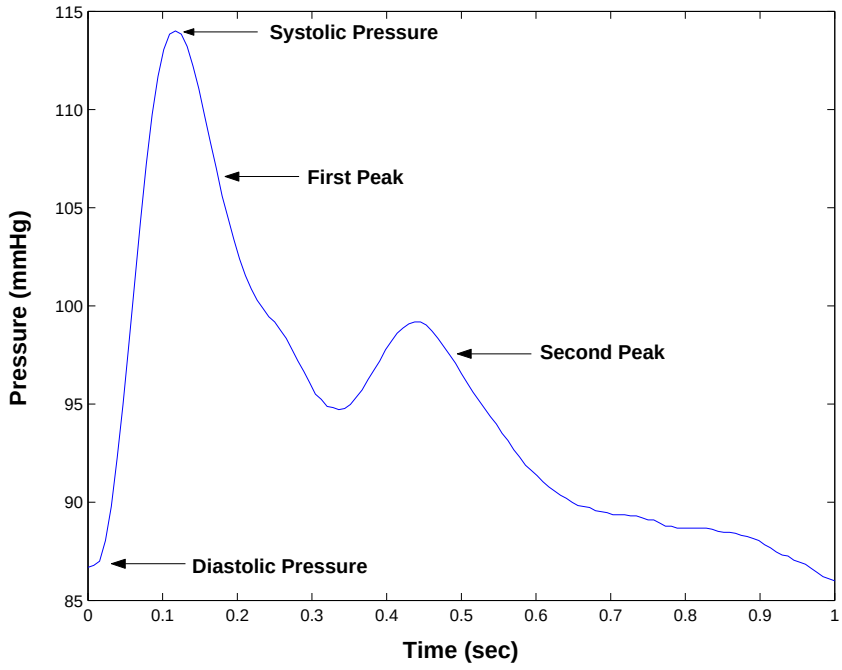


Figure 2.1: Example of pulse wave shape

An artery exhibits the properties of a transmission line and as such can be modeled to have an input impedance and a characteristic impedance. In a network of vessels the input impedance is a ratio of pressure to flow, and can be described by a complex number $\bar{Z}_i(\omega)$. The magnitude of $\bar{Z}_i(\omega)$, which is expressed in Equation 2.1 is the amplitude ratio of pressure and flow [22].

$$\left|\bar{Z}_i(\omega)\right| = \left|\frac{\bar{P}_i(\omega)}{\bar{Q}_i(\omega)}\right| \tag{2.1}$$

The characteristic impedance is defined as the input impedance of an infinitely long straight tube with constant properties. In this case the input impedance will be independent of position and dependent only on vessel and fluid properties. The magnitude of the characteristic Impedance Z_0 is given by Equation 2.2 [22].

$$|Z_0| = \frac{\rho c}{A} \tag{2.2}$$

where A = the cross-sectional area of the vessel, c = wave propagation velocity and ρ = blood density.

The characteristic impedance can be used to determine the size of the reflected wave. These wave reflections occur at points where the properties of the arteries change, and hence the characteristic impedance changes, such as a split in the arterial path.

The velocity of the wave propagation c is affected by the elasticity of the artery and is approximated by the Moens-Korteweg relationship given in Equation 2.3 [21, 22].

$$c = \sqrt{\frac{Eh}{2\rho r}} \tag{2.3}$$

where E = wall elastic modulus, h = wall thickness, ρ = blood density and r = vessel radius.

2.2.1 Wave Reflection

In an arterial system, the input impedance of the vessel varies with changes in the vessel's size and properties. For compliant arteries, which have more elasticity, the wave propagation velocity would be small (Moens-Korteweg Relationship) and hence the Characteristic Impedance would be lower. In rigid arteries the propagation velocity is greater, resulting in a higher impedance. This change in impedance will affect the Reflection Coefficient [22].

Wave reflections occur at arterial junctions where the input impedances of a parent and daughter vessel do not match. The reflection is expressed in terms of a Reflection Coefficient R. The Reflection Coefficient is a ratio of the reflected wave amplitude to the incident wave amplitude and is related to the relative characteristic impedance of the vessels at the junction. In the case where a vessel splits from a primary artery into two branches with different impedances the Reflection Coefficient is given by Equation 2.4 [22].

$$R = \frac{Z_0^{-1} - (Z_1^{-1} + Z_2^{-1})}{Z_0^{-1} + (Z_1^{-1} + Z_2^{-1})} \tag{2.4}$$

where Z_0 is the characteristic impedance of the primary artery and Z_1 and Z_2 are the characteristic impedances of the branched arteries.

The reflection coefficient at each branch point for the arterial system is usually less than 0.2, however, as these coefficients accumulate the overall reflection becomes much greater [22]. The reflected wave augments with the incident wave to produce the characteristic wave shape, which is shown in Figure 2.1. This augmentation produces additional load on the heart, which is characterised by the augmentation index (AiX) [23].

2.2.2 Augmentation Index

The Augmentation Index (AiX) is a measure of the amount of reflection the pressure wave experiences. This reflection translates into additional load on the left ventricle. AiX is the difference between the second peak and the first Systolic peak (As shown in Figure 2.1) as a percentage of ascending aortic pulse pressure (Equation 2.5) [23].

$$AiX = \frac{second\ peak\ -first\ peak}{systolic\ pressure\ -\ diastolic\ pressure} \times 100 \tag{2.5}$$

AiX depends upon heart rate, Pulse Wave Velocity (PWV) and the amplitude of the reflected pulse [23]. In a younger patient, whose arteries are more compliant, the PWV is slower, so the reflected wave arrives at the heart after the aortic valve has closed. In such a case the additional load on the heart is small or absent. In older subjects, where the arteries are stiffer, the PWV is much higher. This results in the reflected wave arriving at the heart before the aortic valve closes, and creates additional load on the heart.

The AiX is calculated from the central aortic pulse wave shape [8, 23]. Measuring the aortic pulse is a complex process and can only be performed using invasive methods. This problem is solved by applying a transfer function to a measured peripheral wave, such as the radial, femoral or the carotid artery. Commercial devices, such as the Sphygmocor system, use a generalised transfer function to calculate the aortic wave shape [19].

2.2.3 Aortic Pulse Estimation

The aortic waveform is generated from the radial or carotid artery using a generalised transfer function. This process can be seen in Figure 2.2. This

approach is used in the Sphygmocor VX (Atcor Medical, Sydney, Australia) and assumes one function for the arterial system for any condition [1]. This is of concern since the arterial system changes with age, therapy and various arterial conditions. Even with these differences, O'Rourke's research [1] shows that this approach is successful with more than 90% accuracy (athough the author does not define this accuracy).

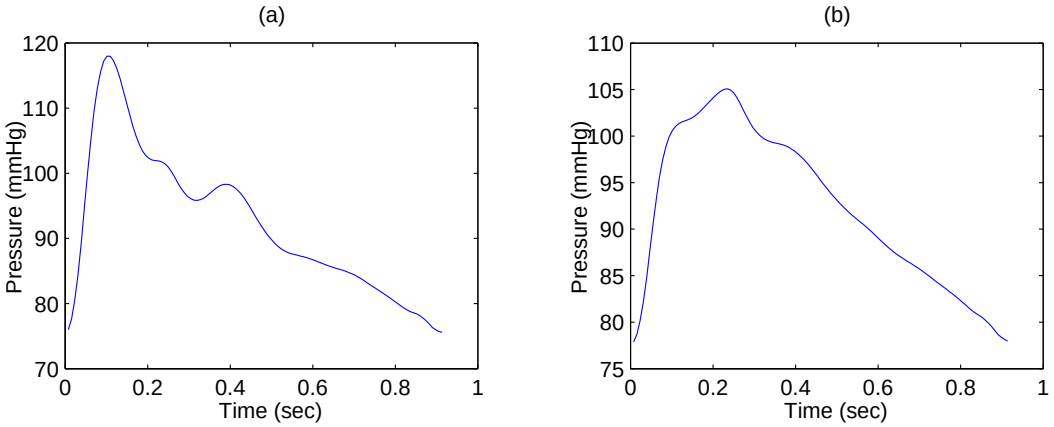


Figure 2.2: Radial to aortic estimation. (a) measured pulse from radial artery using the Sphygmocor system; (b) aortic pulse estimated by a transfer function on the Sphygmocor system.

The problem with this approach is the validation of the transfer function. Segers et al [13] showed that the generalised transfer function led to discrepancies between the synthetic pulse contour and the measured pulse contour. Their study used transmission line theory to develop a transfer function that can be individualised by changing the patients characteristics (age, blood pressure, etc). This approach used a model that was too simple and their results showed that it was not possible to calculate an individualised function.

Millasseau et al [10] determined that the transfer function neither added nor subtracted information contained in the radial pulse. They concluded that the transfer function is of limited value in estimating the effect of central arterial wave reflection, and the same information could be obtained directly from the radial pulse. The developers of the Sphygmocor system responded to this

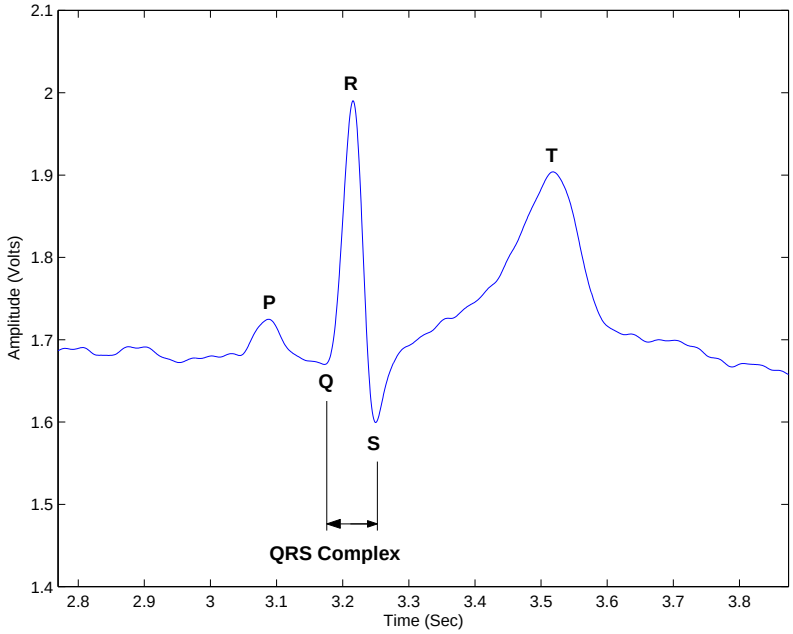


Figure 2.3: An electrocardiograph illustrating the QRS complex

study by saying that the comparisons were limited [24].

2.3 Electrocardiogram

An Electrocardiogram (ECG) was developed for use as a timing signal. This section will touch on an explanation of the ECG, and show how it is associated with the arterial pulse.

The electrocardiograph is a recording of the electrical activity generated by the heart, measured on the body's surface. The ECG is the measured voltage difference between the active (depolarised) area and the inactive (polarised) area of the heart. The waveform is made up of five deflections (sometimes six). These deflections, when present, are designated by the letters P, Q, R, S, T, and U. An example of an ECG wave, measured using a Lead I configuration, can be seen in Figure 2.3. Waves P, R, T and U are usually positive (peaks), while waves Q and S are usually negative (troughs) [20].

The most important feature of the ECG for the present study is the QRS complex. This represents the depolarisation of the ventricles [20]. The QRS complex is used as the timing /gating mark for the pulse contours. This allows the pulse contour to be recorded at different sites separately and aligning the contours together using the ECG signal. This method is the approach used in the Sphygmocor system [19] in order to calculate pulse wave velocity, and eliminates the need to record the pulse contour at two sites simultaneously, which has proved to be difficult [25, 26].

2.4 Measurement Techniques

Pulse wave analysis requires accurate recordings of the arterial pulse. There are two approaches for measuring the wave shape of the arterial pulse, viz - invasive and non-invasive assessment. Invasive techniques involve measuring the wave shape with the use of arterial catheters. This method is generally only used in high-care or intensive care settings where the operator has extensive medical experience. Non-invasive readings are easier to retrieve as they can be performed outside of a hospital and do not involve any needles or injections. Measurements are taken from the surface of the skin, using various techniques. The most popular non-invasive techniques, which are explained in detail in the subsequent sections, are:

- Arterial Tonometry,
- Photoplesymography,
- Doppler Ultrasound,
- Korotkoff Sounds,
- Oscillometry.

Korotkoff sounds and oscillometry only measure the systolic and diastolic pressures and not the full pulse wave.

2.4.1 Arterial Tonometry

Arterial tonometry is based on the method of applanation tonometry, which was originally used to measure the pressure on the retina of the eye. Arterial tonometry is performed by placing a transducer over the artery and depressing the sensor to "applanate" (flatten) the artery. The sensor would have to be re-positioned until a clear pulse is detected. Once the sensor has been positioned the operator applies pressure and the pulse wave shape is recorded. The amount of applied pressure needs to be carefully determined. If the artery is not flattened sufficiently the sensor will measure the forces of the arterial wall tension and the bending of the artery, and if too much pressure is applied, the sensor would occlude the blood flow [22]. Arterial tonometry provides a recording of the full pulse profile, however, it does not provide a calibrated pressure. The waveform is subsequently calibrated to the blood pressure, measured with a cuff sphygmomanometer [1, 22].

Most of the studies that use arterial tonometry make use of a piezoresistive pressure sensor to measure the pulse. Other methods such as using Bragg grating sensors in an optical fibre have been studied [27]. The present research uses piezoresistive pressure sensors for pulse measurement. Arterial tonometry has been used in studies for synthesis of the aortic pulse [1, 2, 19], studies into reproducibility of the pulse wave shape [8, 23] and in studies where the validity of the transfer function has been examined [10, 13].

2.4.2 Photoplethysmography

Photoplethysmography uses optical methods (infra-red) to measure the volumetric pulsations of the blood flow [22]. This method is generally applied to the finger, and is most commonly used in pulse oximetry. Very little attention is paid to the waveform received from pulse oximetry [1]. Feneley et al [2] used photoplethysmography as a comparison to arterial tonometry and to synthesise the aortic pulse.

2.4.3 Doppler Ultrasound

Doppler ultrasound uses echo methods to record arterial volume. Van Lieshout et al [3] conducted a study where the pulse wave shape recorded with ultrasound was compared to photoplethysmography. They concluded that the Doppler ultrasound method requires skill and continuous attention to the direction of the ultrasound beam, using audio and visual techniques.

2.4.4 Other Methods

Korotkoff sounds is an auscultatory method, whereby the pulse pressure is determined by the sounds emitted distally from a partially occluded vessel [22]. This method makes use of an inflatable cuff, which is placed around the limb and a stethoscope is placed on the skin overlying the artery just distal to the cuff. The cuff is inflated to about 30 mmHg above the point where the sounds cease. The cuff is slowly deflated until sounds can be heard, which change as the pressure decreases. Initially a tapping sound can be heard, which denotes the systolic pressure. As the cuff deflates even more the tapping sound becomes a slight murmur, and eventually disappears altogether. The pressure at which the sound disappears denotes the diastolic pressure. This is a common method

which is used everyday for cuff sphygmomanometry.

Oscillometry works by compressing the artery with a cuff, and observing the change in oscillations which are produced by the pressure pulse. These oscillations are measured with the use of a pressure sensor, which is situated in the cuff. As the cuff is slowly deflated the characteristics of the oscillations change. It has been discovered that the point at which the oscillations are at a maximum corresponds to the Mean Arterial Pressure (MAP). Systolic and diastolic pressures are found where the oscillations are a fixed percentage of the maximum oscillations [22]. This method is generally used in automated devices.

2.5 Factors Affecting Pulse Wave Shape

The pulse wave shape changes according to physiological changes, medication, disease and lifestyle habits. Although this research is not intended to investigate these changes, an understanding of these factors is required in order to appreciate the relevance of this work.

2.5.1 Physiological Factors

The pulse wave shape can be affected by different physiological conditions. A few of these conditions are briefly explained [1]:

- **Growth and development:** In infants, the arterial pulse contour in the central arteries is the same as the peripheral arteries. There is no second wave in diastole. This is due to the short body length, which causes the reflection wave to arrive sooner at the heart.
- **Age:** In older subjects, the second systolic peak starts to disappear.

This is a result of increased arterial stiffness and hence an increase in PWV. As the pulse increases in velocity the second peak appears closer to the first systolic peak, eventually forming a contour with only one distinct peak.

- **Diet:** Ingestion of food and drink can reduce wave reflection. This alters the wave contour, and the degree of late systolic augmentation [1].

- **Body Height:** The augmentation is dependent on body height, regardless of age. In shorter subjects the augmentation is greater than that of taller subjects.

- **Gender:** There has been a measured difference in pulse contour between male and female populations. This could, however, be due to the difference in height.

2.5.2 Arterial Diseases

Pulse wave velocity has made a large contribution in studies of arterial diseases. These diseases include, but not exclusive to:

- **Arteriosclerosis:** This refers to the thickening and stiffening of the arterial wall [21]. As the arteries stiffen, the pulse wave velocity increases. This results in early wave reflection at the junctions in the arteries. The reflected wave reaches the incident wave quicker and produces Late Systolic Pressure Augmentation, which can result in an increase of 40–50mmHg to systolic pressure in the central arteries [1].

- **Hypertension:** Hypertension is an abnormal increase in the systolic, diastolic or mean arterial pressure, or all three. This is due to increased arterial stiffness and can be monitored using PWA [1]

- **Diabetes Mellitus:** Diabetes mellitus (Type I Diabetes and Type II Diabetes) has been associated with an increase in arterial stiffness [1]. O'Rourke's [1] studies showed that PWA does not aid in the diagnostics of diabetes mellitus. Further research by Cruickshank [6] showed that PWV is a powerful independent predictor of mortality for diabetes.

- **Chronic Renal Failure:** Savage et al [11] conducted an investigation into the reproducibility of PWA on patients with Chronic Renal Failure (CRF). Their study concluded that indices of arterial stiffness, such as AiX and Time to Reflection (TR), which is determined by PWA, can assist in the assessment of CRF.

2.6 Summary

The study of the pulse contour can provide important information, which cannot be determined from only the systolic and diastolic pressures. The different methods of recording the contours have been discussed, with emphasis placed on arterial tonometry, as this is the method used in the present research. Existing studies have shown the importance of the parameters determined by PWA. Certain parameters rely on the use of a transfer function to determine the aortic pulse contour.

Chapter 3

Hardware

3.1 Overview

The procedure undertaken in the present research was to build a measuring device using arterial tonometry, which can be used for pulse wave analysis. The radial pulse of the test subject was recorded using this device and compared to the pulse contour recorded from the Sphygmocor system.

The designed system comprises two sub-systems: The arterial tonometric system and the electrocardiogram system, which are presented in Sections 3.2.1 and 3.2.2 respectively. The system was powered by two 9 Volt batteries, which were electrically isolated from one another. One battery powered the patient side of the circuit while the other battery powered the amplification side. The designed system was tested for compliance against IEC 601–1, the safety standard for medical equipment [18].

To record high quality biological signals, biopotential systems need to satisfy some basic requirements [22]. These include:

- The monitored signal (such as the pressure pulse or the ECG) should

not be influenced by the measurement system,

- The signal must not be distorted by the measurement system,
- The system must offer protection to the subject against any electrical hazard,
- The system must successfully separate the desired signal from the noise and interference.

A data acquisition system (DAQ), based upon the ADSP-21061 Digital Signal Processor (DSP) from Analog Devices was used to capture the signals. The amplified pulse and ECG signals are sampled at 1Khz with a 16 bit resolution. The DSP controls the communication with the computer using a USB connection. Matlab and Simulink are used to visualise and store the pulse and ECG signals.

This chapter covers the design of each of the stages of the electrical design. The design of the amplification, filtering, isolation and detection sections are explained. The complete circuit diagrams are shown in Figure B.8 and B.9 on page 94 and 95 respectively. The circuits are explained in more detail in the Appendix B.

3.2 Design Overview

3.2.1 Arterial Tonometry Design

The arterial tonometry system measures the pulse wave shape by recording the deflection of the skin caused by the pulse pressure. The system made use of a highly sensitive pressure transducer, and necessary amplification and filtering techniques, which are shown in the block diagram in Figure 3.1. The

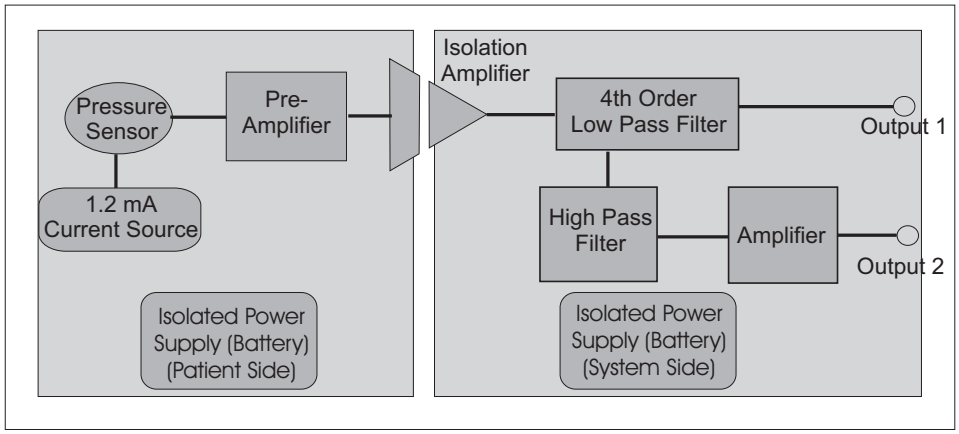


Figure 3.1: Block diagram of arterial tonometry system

tonometry system was housed in two plastic enclosures: One contained the sensor and the sensor amplification and the second enclosure contained the electrical isolation and filtering. The circuit diagram for the sensor unit is presented in Figure B.9 and the circuit diagram for the filtering and isolation circuit is presented in Figure B.8, in Appendix B.

3.2.2 Electrocardiogram Design

The electrocardiogram is a bipolar, AC signal in the range of 0–10mv with a bandwidth of 0.05Hz–150Hz. The ECG provides information over the full range of frequencies. The lower frequencies provide a correct measurement for the slower ST waves while at higher frequencies accurate information about the QRS complex is contained. At this frequency range there are several sources of noise. High frequency noise includes noise due to muscle contractions and low frequency noise includes respiratory noise and baseline drift due to body motion [22]. 50Hz noise was also introduced from surrounding electrical equipment. Amplification and filtering needed to be carefully chosen to obtain a good quality ECG waveform.

Figure 3.2 shows the block diagram of the ECG amplifier. The ECG was

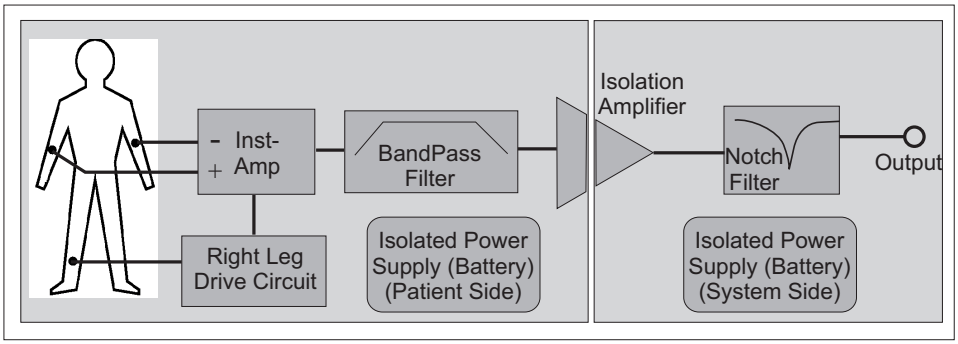


Figure 3.2: Block diagram of ECG amplifier

measured using the Einthoven's 3-lead ECG configuration. A *Lead* is the connection of two biopotential electrodes used to record an ECG [20]. The Lead configurations are shown in Table 3.1. In this study the Lead I configuration was used which connected the left arm (LA) (positive) and the right arm (RA) (negative). Although other Lead configurations were tried, the Lead I produced the best QRS complex, and it was easier and convenient to attach the ECG electrodes to the arms. These two electrodes measured the voltage difference across the heart (LA-RA), which is caused by polarisation and depolarisation. A third electrode was used as a reference point, which was taken from the right leg. This electrode was connected to a circuit known as a right leg drive, which uses a negative feedback loop to reduce the common-mode interference [22]. The Right Leg driver circuit is explained in more detail in Appendix B.2.2.

Lead	**Positive Electrode**	**Negative Electrode**
I	Left Arm	Right Arm
II	Left Leg	Right Arm
III	Left Leg	Left Arm

Table 3.1: Einthoven's 3-Lead ECG configuration

The ECG amplifier was initially built on a dual supply system due to the bipolar nature of the ECG signal. It was subsequently converted to a single supply system to reduce the circuit complexity and to keep it in line with the arterial tonometry system, which was single supply.

3.2.3 Assembly

The majority of the circuit was housed in a plastic box of 120mm×76mm×42mm. The sensor and its pre-amplifier were housed in a smaller box of 50mm×35mm×20mm. The circuit was assembled on prototyping strip-board, which, in hind sight, was a poor decision because the strip-board required additional debugging, and delayed the testing process.

3.3 Signal Detection

Arterial tonometry measures the pulse waveform by recording the deflection of the skin over an artery. This deflection is caused by the pressure pulse, which can be recorded using highly accurate pressure transducers. The pressure transducer is placed on the skin, over the artery, and by compressing the artery slightly with the sensor, the pulse waveshape is recorded.

The pressure transducer used in the design is the IC-Sensor model 84 (IC Sensor, MSI, USA). This is a piezoresistive pressure sensor, packaged in a stainless steel housing. The pressure contact area has a diameter of 19.1mm, and transfers pressure from the diaphragm to the sensor through silicon oil [28]. The transducer has a pressure range of 0–300mmHg, with a full scale output span of 100mV, and zero pressure output of 1mV. The resolution of the sensor is 0.33 mV/mmHg.

The pulse wave shape is measured by gently placing the transducer over the radial artery, in the same way as one would do to feel a pulse. The size of the contact surface therefore plays a big role in the measurement of the pulse. The contact surface area of the Model 84 sensor is significantly larger than that of the Millar micromanometer, which can be seen in Figure 3.3. The larger



Figure 3.3: Comparison of different sensors. The top sensor is the IC-Sensor enclosed in a plastic housing and the bottom sensor is the hand held probe from Millar Instruments, which is used in the Sphygmocor system.

surface area did prove to have definite advantages and disadvantages.

The advantages of the Model 84 Sensor included: increased sensitivity, which allowed smaller deflections to be measured without too much pressure being applied to the artery. This also resulted in no visible pressure marks being left on the wrist once the sensor was removed.

The disadvantage to the larger surface area was that it was clumsy to handle. The Millar micromanometer is the size of a pen and is easy to hold steady while recording was in progress. The larger sensor made it more difficult to hold steady while recording the pulse. Another down side to the larger sensor was the difficulty experienced while trying to find the pulse on subjects with small wrists. In these cases the small bones in the wrist obstructed the site for the pressure sensor.

The Millar micromanometer was used as a reference point as this has been the preferred sensor to use in arterial tonometry research. The Model 84 pressure

sensor was selected because it produced the best results in preliminary tests. Other sensors which have been used for this purpose include the Motorola MPX2300DT1 disposable medical sensor used by Salter and Bird [25], but was not included due to its disposable nature. Current research conducted by The Rand Afrikaans University (RAU), Johannesburg makes use of fibre optics to measure the pulse [27].

3.4 Amplification

3.4.1 Pulse Amplification

The arterial blood pressure can range from Diastolic pressures of 50mmHg up to Systolic pressures in excess of 200mmHg. Non-invasive pressure measurements do not record the blood pressure directly but rather the deflection on the skin caused by the arterial pulse wave. This measurement would not exceed 100mmHg, therefore the full scale of the pressure sensor was not required. The measured pressure range required a minimum amplification of 100, which was achieved using two stages of amplification.

An instrumentation amplifier was used to amplify the signal to a range of 0–5V. The instrumentation amplifier used discrete components, i.e. three op-amps, instead of using a single chip instrumentation amplifier. This method made use of the internal gain set resistor of the pressure sensor. By using the gain set resistor, the interchangeability of the sensor was maintained. However, this approach meant that a single chip instrumentation amplifier (such as the AD623 from Analog Devices) could not be used. In order to maintain a high accuracy and avoid a DC voltage offset, 1% tolerance resistors and precision op-amps were used. The design used Microchip MCP609 amplifiers which have a Common Mode Rejection Ratio (CMRR) of 91dB and an input offset voltage

of 250μV. The instrumentation amplifier provided a gain of 75, which resulted in a pulse amplitude of approximatly 1.5V peak-to-peak. The circuit diagram is shown in Appendix B.2, where it is explained in more detail.

The second stage of amplification was included after the instrumentation amplifier. In order to measure a pulse using applanation a certain amount of pressure must be applied to the artery in order to detect a pulse. This applied pressure creates a DC offset, which can vary. This variation is caused by operator movement, fluctuations between the pressure probe and the artery and the condition of health of the test subject. To remove this offset, the signal is filtered through a high-pass filter with a cut off frequency of 0.3Hz. The output of the filter was the pulse wave shape, with the DC offset removed. This signal was passed through a non-inverting amplifier with a variable gain of between 1 and 10. The end result was a signal that the user could clearly see on the screen, which assisted in recording the best signal. A similar variable gain function is used in the Sphygmocor system, however it is implemented in software and not hardware.

The block diagram in Figure 3.1 shows two outputs. Output 1 is the signal with the applied pressure (i.e. the signal does not go through the high-pass filter and second amplifier). This signal provides a direct measurement of the pressure applied to the artery, which would be used in the analysis of the data. The second output, Output 2, is the result of the second stage amplifier.

3.4.2 ECG Amplification

The electrocardiogram has a voltage range of between 0.1mV–10mV [22]. A preamplifier with a high CMRR and a high input impedance was required for the amplification of the ECG. This was achieved with the use of a AD623 single chip instrumentation amplifier from Analog Devices. The AD623 features a

CMRR of 100dB with a frequency response of 100KHz and is powered by a single-ended power supply. Although Analog Devices recommends the AD620 instrumentation amplifier for an ECG application [29], the AD620 was tested and it was found that the AD623 produced greater amplification with less noise. The AD620 also required a dual supply system which created a problem in the system which was primarily single supply. The instrumentation amplifier provided a differential gain of 12.14 (see Appendix B.2).

A right leg driver circuit was used to provide a reference potential for the ECG amplifier. The drive circuit amplified the common mode interference in an inverting amplifier and fed the output back into the circuit as the reference electrode. This inverted common mode voltage reduced the common mode interference of the amplifier [22].

The signal was then filtered using a bandpass filter, which is explained in Section 3.5. A second amplifier stage, which formed part of the bandpass filter, was included in the design. A non-inverting amplifier with a gain of 40 was used. The overall gain of the ECG amplifier was 485. This produced an output voltage range of 0–1.5V.

The full circuit diagram of the ECG amplification is presented and explained in Appendix B.2.

3.5 Noise Reduction

A medical environment provides a number of sources for noise, but the majority of noise is 50Hz line interference [22]. In the case of the arterial tonometry system the main sources of noise are high frequency noise ($>$ 200Hz) and 50Hz line interference. The isolation amplifier reduced a lot of the high frequency noise, but did not remove the 50Hz line interference. A fourth order, analogue,

low-pass Butterworth filter with a -3dB point of 40Hz was used. This filter, shown in Figure B.4 in Appendix B, reduced the 50Hz noise, but also reduced the bandwidth of the pulse signal to 0–40Hz.

A high pass filter with a cut off frequency of 0.3Hz was included after the low pass filter. This filter removed the DC offset which is caused by the constant pressure applied to the wrist. This did cause a problem in that as soon as the pressure was released the signal would saturate to ground, and then only after a short period of time return to the reference point. The values for the RC network were chosen to keep the time constant low, however, this did increase the cut-off frequency.

The ECG potential suffers from the same noise problems as the arterial pulse as well as additional noise. Noise is introduced by surrounding equipment as well as biophysical interference caused by respiration or muscle contractions [22, 30]. A bandpass filter is used to attenuate high frequency noise as well as to remove the DC offset and baseline drift [22]. The bandpass filter, which is presented and explained in Appendix B.3, comprises a first order high pass filter (HPF) with a cutoff frequency of 0.05Hz and a first order low pass filter (LPF) with a cut-off frequency of 100Hz.

A Twin-T notch filter was used to attenuate the 50Hz line interference in the ECG circuit. The filter comprises a first order high pass and first order low pass filter whose frequencies are exactly matched to 50 Hz. The circuit diagram and explanation can be found in Appendix B.3. The results of the notch filter are evident in Figures 3.4 and 3.5, which show an ECG trace before and after a notch filter was added.

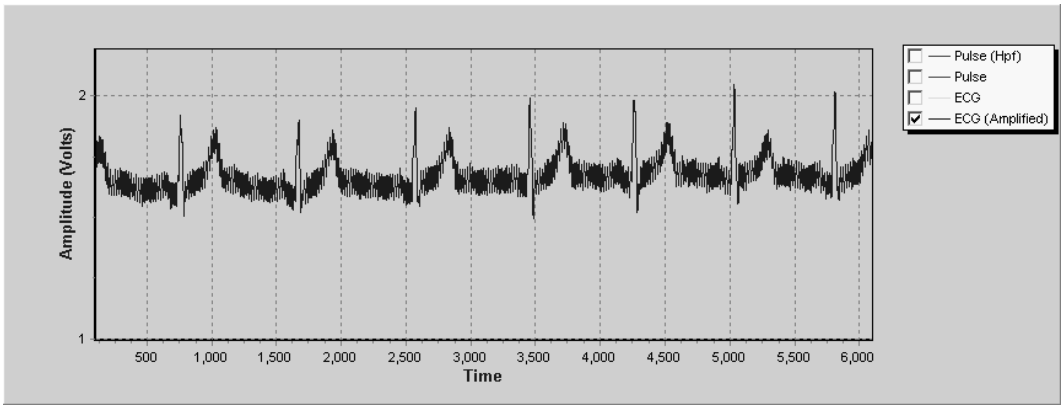


Figure 3.4: ECG trace without a notch filter

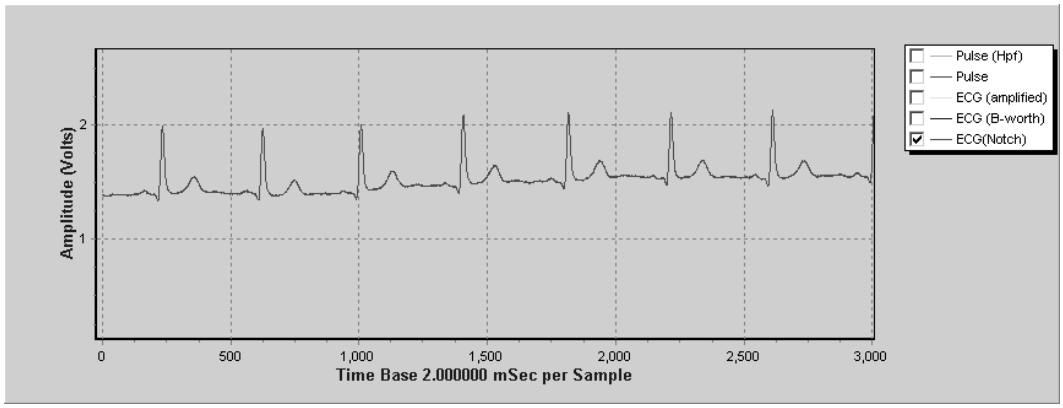


Figure 3.5: ECG trace with a notch filter

3.6 Patient Safety and Isolation

Patient safety needed to be taken into consideration in the design of the pulse amplifier and the ECG amplifier. This was achieved by focusing on two aspects, namely by using a battery power supply and electrical isolation.

3.6.1 Electrical Isolation

Electrical isolation can be achieved with the use of isolation amplifiers. An isolation amplifier is required to break ground loops and provide isolation protection to the patient and electronic equipment [22]. The main purpose of the isolation amplifier is to protect the patient by eliminating the hazard of electric shock, which could be caused by leakage currents flowing to ground through the patient under a fault condition [18, 22]. Even though both the ECG system and the arterial tonometry system were battery operated, the system was connected to a computer and the DAQ system which were both powered by a mains supply (230VAC). The isolation amplifiers were used to safeguard the patient from any possibility of leakage currents caused by the DAQ or computer.

Isolation amplifiers are defined by Isolation Mode Rejection Ratio (IMRR), which is the ratio between the isolation voltage and the output voltage of the amplifier. The typical value of IMRR for medical equipment is 140dB at DC and 120dB at 60Hz, with an isolation impedance of $1.8\text{pF}\|10^{12}\Omega$ [22].

The design used opto-coupling isolation methods since the amplifiers are small, easy to use and can transmit low frequencies [31]. Two different opto-coupling isolation amplifiers were tested in the research. These are presented in Table 3.2 and the test results are explained.

Table 3.2: Tested opto-isolation amplifiers

Opto-Isolator	**Isolation Voltage (V_{ISO})**	**IMRR**	**Impedance**	**Ref**
HCPL7800	3750 V	>140 dB	$\geq 1 \times 10^{12}$	[32]
4N28	3750 V	Not Specified	1×10^{12}	[33]

The HCPL7800, which is a digital opto-coupler, was first tested in the circuit. The signal was first digitised, and then transmitted from the patient side to the circuit side using an optocoupler. The digital stream was converted back to an analogue signal and outputted. This amplifier was tested and the output signal was found to be extremely noisy. It was also found that a DC offset was introduced in the output signal. In two different cases an offset of 600mV and -250 mV were introduced.

The second isolation amplifier that was tested was the 4N28. This is simply a matched photo diode and photo transistor. The 4N28 is defined by the Current Transfer Ratio (CTR), which has a typical value of 100%. The current was controlled by a resistor in series with the diode and by a resistor in series with the emitter of the transistor. By varying the value of these resitors, the signals were transmitted accross the isolation barrier without causing any saturation. The circuit diagram and explanation are presented in Appendix B.4.

3.7 Testing and Calibration

3.7.1 Electrical Safety Compliance Test

The device needed to be tested and calibrated before use. The most important test was the electrical safety. The device was classified by the IEC 601-1 standards as a Class I device and had to meet the specifications described in Section 1.4.

Electrical safety was tested with the use of a certified test-bed specifically designed to test compliance of IEC 601-1 standard. The testing was conducted by Brittan Health Care (Johannesburg, South Africa) and the results of these tests can be found in Appendix D. The patient auxiliary current was checked on all of the electrode leads as well as the contact surface of the pressure sensor. In the case of the ECG, all the leads measured a patient auxiliary current of less than 3μA at DC. The maximum limit is specified at 10μA [18].

The earth resistance of the full measurement system (computer, DAQ and sensors) was tested according to IEC 601-1 standards. Even though the system was powered by batteries there was still the possibility of the leakage currents from the DAQ or computer finding a path to ground through the patient. This problem was prevented with the use of the isolation amplifiers. The earth resistance of the system was measured at 3Ω, well within the 200Ω specification.

3.7.2 Sensor Calibration

The complete pulse amplification system was tested and calibrated to determine the linearity of the amplified signal. This was achieved by attaching a modified cuff sphygmomanometer to the pressure sensor and measuring the voltage output as the pressure increased. The manometer's pressure was increased in increments of 5mmHg ranging from 0mmHg to 110mmHg. The voltage was recorded at the output of the Butterworth filter, and the results can by seen in Figure 3.6. This calibration provided an indication of the pressure that was applied to the wrist. It did not provide a calibration for the pulse wave, which was performed in software instead.

$$Non\ Linearity = \frac{\hat{N}}{O_{MAX} - O_{MIN}} \times 100\% \tag{3.1}$$

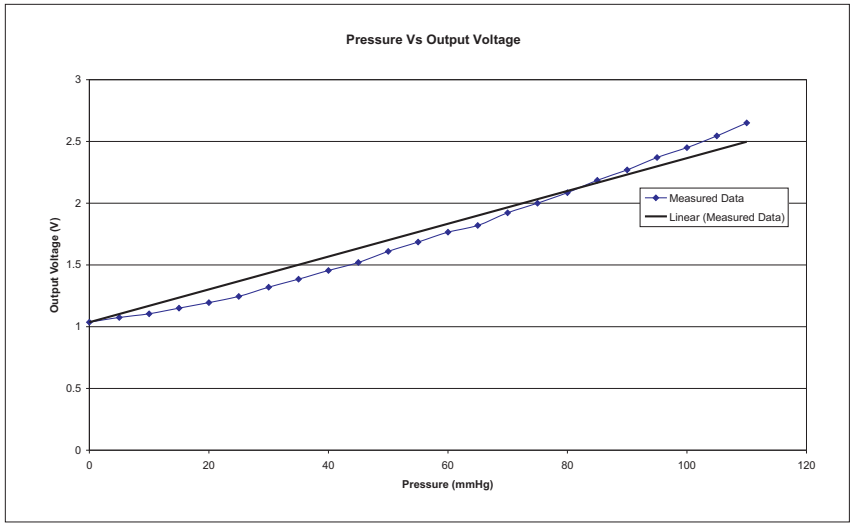


Figure 3.6: Calibration curve of system

The non-linearity of the system is calculated between 0 mmHg and 110 mmHg by Equation 3.1 [34], where $\hat{N}$ is the maximum non-linearity and O_{MIN} and O_{MAX} define the output range. The overall pulse system exhibits a non-linearity of -11.43% between 0 and 110mmHg. The graph also exibits an error between 0mmHg and 80mmHg, which is greatest around 20–40mmHg. This error provided early indication that the design of the sensor may be flawed. Since the curve shown in Figure 3.6 was not used to calibrate the pressure pulse, the cause of this error and non-linearity was not invetigated further.

3.8 Data Acquisition

The data was captured and recorded onto a computer using a Data Acquisition System (DAQ) which was developed at The University of the Witwatersrand, Johannesburg. The DAQ is based on the ADSP-21061 Digital Signal Processor (DSP) from Analog devices. The DAQ communicated with the computer via Matlab and Simulink using software that had already been developed for data acquisition, which received the data from the DSP through a USB connection.

Three signals were sampled using the DAQ system: One ECG signal and

two pressure pulse signals (one filtered and one unfiltered). The signals were sampled using an analogue-to-digital converter (ADC) with a 16-bit resolution and at a sampling frequency of 1KHz. Offsets of 4 and 7 volts were added to the unfiltered pulse and ECG respectively, using a Simulink model. These offsets allowed the user to view all three pulses simultaneously without any of the traces overlapping one another on the screen. The data was recorded in 10 seconds segments and stored in the Matlab workspace, where it was analysed further.

Chapter 4

Testing and Data Analysis Methods

4.1 Overview

The signals retrieved from the designed arterial tonometry system were validated by testing the system on a small group of test subjects. The following chapter explains the testing procedure, the ethics requirements and the methods used to analyse the data. Different approaches were used in the analysis which have been explained and compared in this chapter. The results of the tests are laid out in Chapter 5.

4.2 Measurement Procedure

The arterial tonometry device was tested by doing a comparative analysis on nine test subjects. The subjects' characteristics are detailed in Table 4.1. Subject 2 was discarded because there was a problem with recording the data. The

testing was conducted at the School of Physiology, University of the Witwatersrand, under the supervision of Professor Gavin Norton.

No.	Sex	Age (yrs)	Blood Pressure	
			SBP(mmHg)	DBP(mmHg)
1	M	30	130	78
2	F	26	122	80
3	M	54	134	90
4	M	33	130	82
5	M	25	120	78
6	F	28	118	76
7	M	36	124	82
8	M	63	250	92
9	F	45	114	76
Mean		38	138	82
STD		13	42	6

SBP = Systolic Blood Pressure
DBP = Diastolic Blood Pressure

Table 4.1: Subject characteristics and clinical results

The procedure for testing was as follows:

1. Record the subject's blood pressure using a cuff sphygmomanometer,
2. Record the waveform of the radial artery using the Sphygmocor system,
3. Record the subject's ECG using the designed system,
4. Record the waveform of the radial artery using the designed arterial tonometry system.

The first two steps of the procedure were conducted by a trained operator who has expert knowledge of the Sphygmocor system. The measurements using the designed system were conducted by a different operator, who was more familiar with the designed system.

The pulse waveform is measured in the same way as feeling for a pulse on the wrist. The pressure sensor is placed on the wrist, over the radial artery. The location of the sensor for each system can be seen in Figure 4.1.

The pulse wave shape was recorded for eight of the nine subjects. The data for Subject 2 was discarded since a clear pulse wave shape could not be recorded. The pulse wave shape was recorded for the remaining eight test subjects, however the quality of the recordings varied. The reasons for this variability have been outlined in Section 5.2. An example of a recording is shown in Figure 4.2, where it can be seen that the pulse from the Designed system saturate at zero volts. This was caused by an insufficient DC offset. The full set of recorded data from all nine subjects can be found in Appendix C.

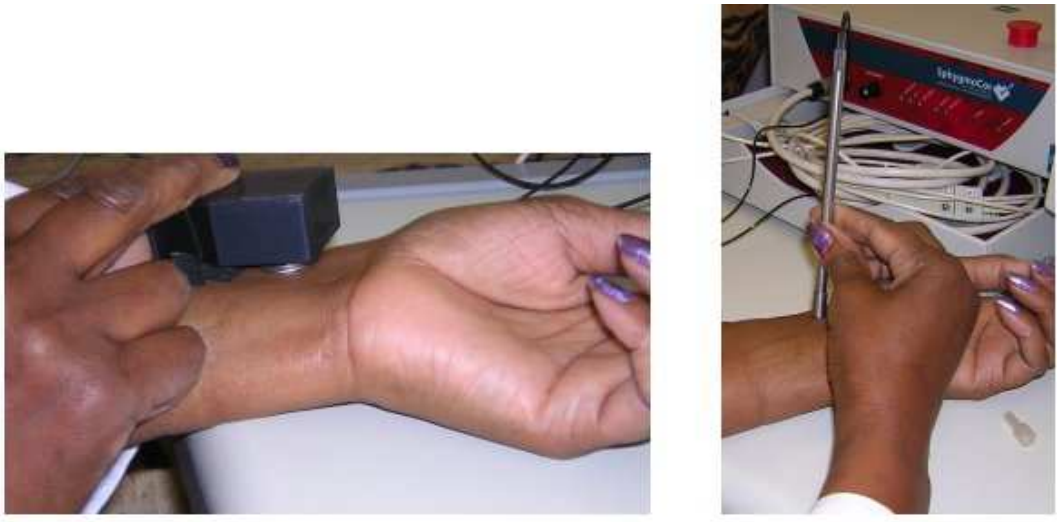


Figure 4.1: Location of pressure transducers on the wrist; (a) designed system and (b) Sphygmocor System

4.2.1 Ethics Approval

Before any tests could commence ethics approval was obtained from the Human Ethics Research Committee at The University of the Witwatersrand, Johannesburg. The code of ethics requires that the research is safe and ethical and that the rights of the test subjects are respected. All the test subjects were properly informed about the research and testing methods and testing did not commence without their written consent. The information sheet and

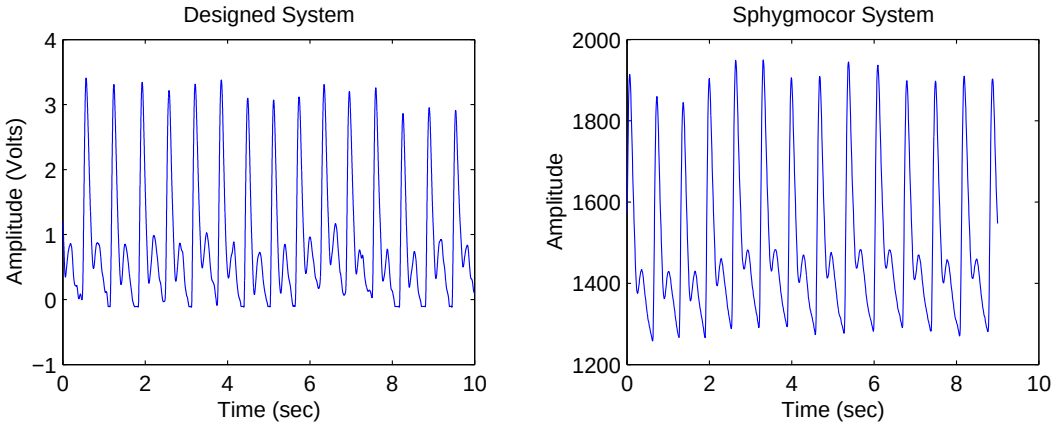


Figure 4.2: Ten second recording of pulse measured from both systems

consent form as well as the Certificate for Ethics Approval can be found in Appendix 4.2.1.

4.3 Data Preparation

4.3.1 Signal Enhancement

The recordings of the pulse wave shapes were retrieved in intervals of 10 seconds, as shown in Figure 4.2. Any high frequency noise, which was not removed by the analogue filters was removed before further analysis took place. This was done with a digital infinite impulse response (IIR) Butterworth filter. The filter was designed, using Matlab, with a 50Hz cutoff point and a roll off of -60dB at 150Hz. To prevent any phase shift a zero phase shift filter was used. The filter was applied to both the ECG signal and the pulse signal. Once the high frequency noise was removed, the signal was divided into individual pulses and calibrated to the pulse pressure.

4.3.2 Pulse Wave Calibration

The data received by the Sphygmocor system was scaled differently to the data from the designed arterial tonometry system. Data from both systems were calibrated to the range of the pulse pressure. The pulse wave shape was scaled to the pulse pressure but careful attention needed to be taken to prevent the signal from distorting. In a single pulse recording the maximum peak can vary even though the systolic pressure is constant. This variation is related to the movement of the pressure sensor and not to the actual pulse pressure changing. By measuring this variation the performance of the pressure transducer can be measured. If the signal was distorted this measurement would be incorrect.

To avoid distortion, the pulse signal is calibrated with reference to the average of all the individual pulses of a particular subject (i.e. a period of the waveform). Figure 4.3 shows the average pulse and the individual pulses where the systolic peaks have not been distorted.

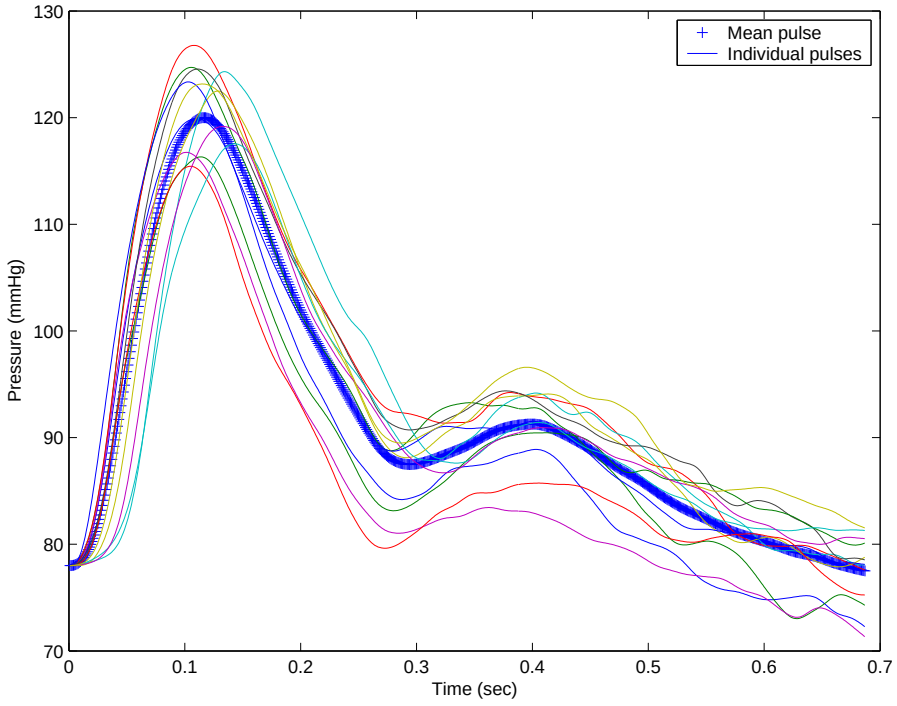


Figure 4.3: The individual pulse periods calibrated with respect to the average pulse

The algorithm used to calibrate the waveform is as follows:

1. Remove the DC offset by subtracting the value of the foot of the pulse. (Estimation of the foot of the pulse is explained in Section 4.4),
2. Scale the pulse by a ratio of pulse pressure to the mean value, i.e. $(\times \frac{systolic\ pressure - \ diastolic\ pressure}{max(avg\ pulse) - foot(avg\ pulse)})$
3. Shift the pulse by the value of the diastolic pressure.

4.4 Pulse Foot Identification

The recorded signals from both systems displayed some DC drift, which made it difficult to analyse the complete pulse signal. Since the pressure pulse is a periodic signal, as shown in Figure 4.2, the signal could be divided into its individual pulses to assess the quality of the recording. This was performed using three different methods. The starting point of the individual pulses needed to be consistent to ensure that any time-domain comparisons were accurate. If the location of the foot of the pulse varied for each pulse, the systolic rise time and any subsequent time measurement would have been false.

There are four methods which have been used to identify the foot of each pulse [35], these include:

1. The point of minimum diastolic pressure,
2. The point where dP/dt is a maximum (The sharp upstroke of the pulse waveform),
3. The point where the second derivative is a maximum,
4. The point where the line tangent of the initial upstroke and the horizontal line through the minimum point intersect.

Chiu et al [35] concluded that method 3 and 4 yielded the best results for invasive and non-invasive methods, with a correlation coefficient between data of greater than 0.9. The approach taken for the present research was to test methods 1 and 3 as well as an additional method of using the peak of the QRS complex (defined in Section 2.3 on Page 27) of the ECG as the start of the pulse period. The three different algorithms were tested on the pulse signals to determine which method was the most efficient in identifying the individual pulses. The different methods were compared by analysing the individual pulses with respect to the mean value of the pulses. This was achieved using three diagnostic measurements, which were:

- The time difference (τ) between the systolic peak of each pulse and the systolic peak of the mean pulse. This was affected by the location of the foot of the pulse. If the diastolic foot is consistent, the time difference will be minimal.
- The Correlation Coefficient (CC) between each individual pulse.
- The Root Mean Square (RMS) error between the average pulse and each individual pulse.

The results from the three different methods are presented in Chapter 5. The algorithms for each method are described in the next three sections.

Method 1: Point of Minimum Diastolic Pressure

The method of finding the minimum diastolic pressure is as follows:

1. Determine the middle point of the systolic upstroke by finding the maximum of the first derivative dP/dt,

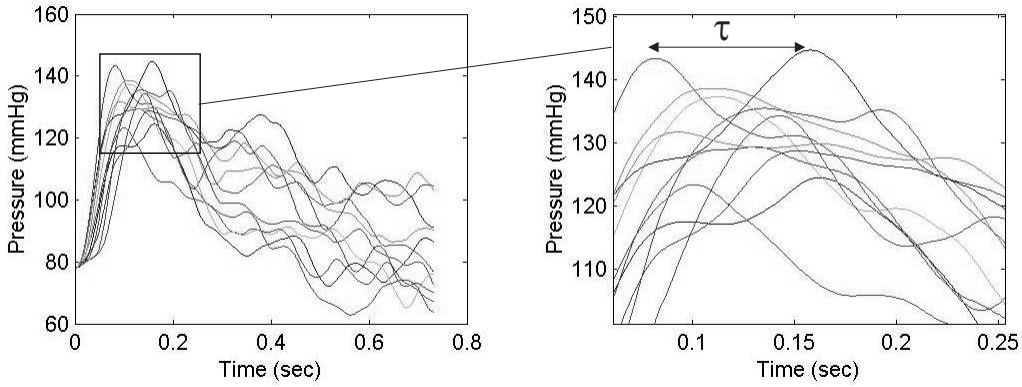


Figure 4.4: Time variation of Systolic peak

2. Identify the point of maximum dP/dt for each systolic upstroke by increasing the range of the search criteria by 2 $\times$ standard deviation of dP/dt

3. Using a search algorithm, find the first trough preceding each point of maximum derivative. This point marks the foot of each pulse.

This method was the most successful for separating the wave into individual pulse periods. Only one set of data out of nine sets could not be separated. The disadvantage of this method was the large variation in the time between each individual pulse (τ), which can be seen in Figure 4.4. Method 1 produced the largest error for the time variance of the systolic peak (5.36 $\pm$ 22 ms). An example of the results from method 1 can be seen in Figure 5.2 (a)

Method 2: Point of Maximum Second Derivative

Two different algorithms were used to determine the foot of the pulse by maximum d^2P/dt^2. The first attempt used a simple algorithm that determined the maximum value of d^2P/dt^2 within a limited range. This algorithm had a poor success rate of only 50% . The second attempt was more involved and had a 90% success rate. The successful algorithm is as follows:

1. Determine the point of the maximum of the first derivative as explained in the Method 1.

2. By working backwards along the curve of d^2P/dt^2, from the point of maximum dP/dt, the maximum of d^2P/dt^2 is found

3. Identify all the pulse periods and separate the wave into individual pulses as shown in Figure 5.2 (b).

The correlation between the individual pulses showed an improvement from that of Method 1. The correlation coefficient (0.90 ± 0.09) correlates with Chiu's [35] findings for this method. The time variance of the systolic peaks showed an improvement (-0.86 ± 17.5 ms), however the RMS error has increased (11.3 ± 6.02 mmHg).

Method 3: Using the R wave of the ECG

This method makes use of the ECG signal that is recorded simultaneously. The QRS complex of the ECG, which is generally much greater in amplitude, is used as the timing mark. This provided a consistent point to mark the start of each individual pulse, which can be seen in Figure 5.2 (c). This method relies on a good quality ECG signal recording to successfully identify the start of each pulse. This was not the case for two of the tests subjects who had poor or irregular ECG recordings. The time variance (τ) showed only a slight improvement on Method 2 (-0.67 ± 14.6 ms). The correlation coefficient and RMS error were worse than those of Method 1 and Method 2.

4.5 Performance Analysis

4.5.1 Pulse Wave Quality

A good quality signal is required for an accurate assessment of the arterial system. The quality of the signal from the designed system was assessed and compared with the quality of the Sphygmocor signal. The aim was to determine the reproducibility of the waveshape using the designed system.

The quality of the full recording of 10 seconds is assessed by separating the pulse signal into the individual pulses and comparing these to the average pulse. The pulse signal from both systems are separated using the second derivative method (method 2) as described in Section 4.4. This method was chosen since it produced the best results for correlation coefficient and RMS Error (Table 5.1) and it is the default method used by the Sphygmocor system [35]. An example of the individual pulses retrieved from the designed system and the Sphygmocor system can be seen in Figure 4.5(c & d) respectively. The full set of results can be found in Appendix C.1

This analysis was performed on the results from the designed system and the Sphygmocor system. The results retrieved for the designed system are compared against the results for the Sphygmocor system. In both cases the average pulse for each system is taken as the point of reference, and is calculated by Equation 4.1 [34],

$$\bar{y} = \frac{1}{N} \sum_{i=1}^{i=N} y_i \tag{4.1}$$

where N is the number of pulses per ten second recording ($N = 13$ for Figure 4.5(a)) and y_i are the sampled data points of the pulse.

The signal is assessed by comparing key points on each of the average pulses. These points, which were used in the study by Fetics et al [36] to compare

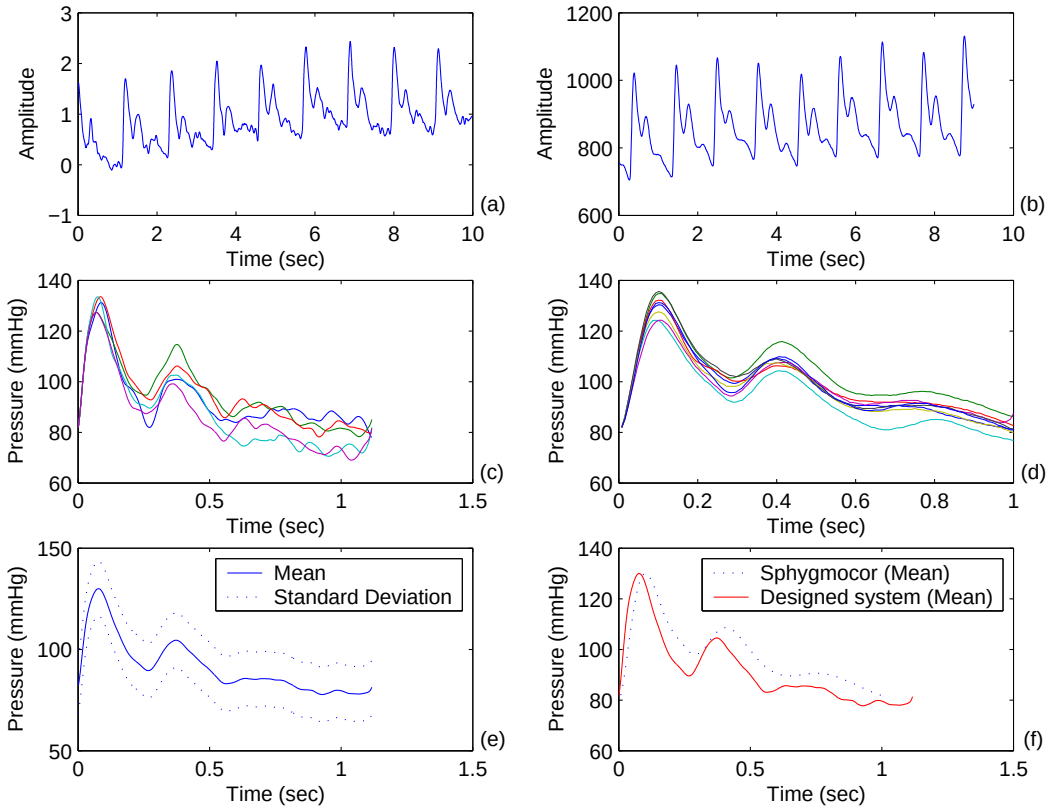


Figure 4.5: Example of recorded data: (a) pulse signal measured using designed System; (b) pulse signal measured using Sphygmocor system; (c) separated pulse from designed system; (d) separated pulse from Sphygmocor system; (e) Mean (solid line) and standard deviation (dashed line) of pulse from designed system; (f) comparison of pulse of the designed system and the Sphygmocor system

the radial artery wave shape with an estimated aortic artery wave shape, are labeled in Figure 4.6 and are explained in the following paragraphs. They include:

Error in Systolic Pressure

The error in the systolic pressure was calculated as the difference between the peak of each pulse and the systolic blood pressure. The systolic blood pressure was measured using the Sphygmomanometer.

Error in Systolic Rise Time

The error in the systolic rise time provided an indication of the consistency of the pulse foot. The error is calculated as the difference between the individual pulse and the mean pulse.

Correlation Coefficient

The correlation coefficient provides a measure as to how close each pulse is related to the next. For a good quality signal each pulse must be as closely related as possible to the next and should be above 90% correlation [37]. The correlation coefficient , r, between signal x and y is obtained from

$$r = \frac{\sum_{i=1}^{n}(x_i - \bar{x})(y_i - \bar{y})}{\sqrt{\sum_{i=1}^{n}(x_i - \bar{x})^2}\sqrt{\sum_{i=1}^{n}(y_i - \bar{y})^2}} \tag{4.2}$$

where $\bar{x}$ and $\bar{y}$ are the mean values calculated using Equation 4.1.

Root-Mean-Square Error

The Root-Mean-Square (RMS) error was calculated for each pulse with respect to the mean pulse. The equation for RMS error is given in Equation 4.3 [38]. To test the signal quality the *Actual* value is equal to the mean value. This results in the RMS error being equivalent to the standard deviation of the pulse. An example of the standard deviation (RMS error) of a single pulse can be seen in Figure 4.5(e). To avoid confusion in the following chapters, the notation for the RMS error is RMS_{std}.

$$Error_{RMS} = \sqrt{\frac{\sum (Actual \ - \ Predicted)^2}{Number \ of \ Predictions}} \tag{4.3}$$

The results of the quality tests are expressed as mean ± SD, and are presented in Chapter 5.

4.5.2 Sphygmocor Comparison

The second test was to compare the signal between the Sphygmocor and the designed system. Unfortunately the large fluctuations in the recordings prevented any meaningful comparisons between the full 10 second recordings measured form the two systems. The cause of these fluctuations are described in Section 5.2. Due to the high variability of the recordings from the designed system, all the comparisons were performed using the average of the pulses from both systems, calculated using Equation 4.1. The data from the Sphygmocor was interpolated from 128Hz to 1000Hz in order to match the sampling frequency of the designed system. A FFT interpolation algorithm was used for this purpose.

The aim of this test was to compare the readings of the designed device with that of the Sphygmocor system. The problem arose that even though the Sphygmocor system is the leading system in this field of measurement its weakness is in its validation [1]. Several studies [1, 8, 10] have been performed to determine the reproducibility of the the pulse wave velocity and the augmentation index and the validation of the transfer function as calculated by the Sphygmocor system. With no set standard and reference point for this type of measurement, the Sphygmocor was assumed to be a true point of reference.

The pulse signals from the two systems were compared by analysing three points on the curve as well as the RMS error between the two pulses [36]. The three points, as seen on Figure 4.6, were the systolic peak, the second systolic peak and the dicrotic notch. An example of the comparisons is shown in Figure 4.5(f). The result of the comparisons are discussed in Chapter 5,

and the full set of results can be found in Appendix C.

Systolic Peak

The most common measurement for blood pressure is the systolic and diastolic pressures. If the systolic peak is not recorded correctly, or is distorted by the measuring system this would result in an incorrect assessment of the pulse rate and blood pressure.

The error in systolic pressure is calculated as the difference between the mean pulse and the systolic pressure measured from the Sphygmomanometer. The error in the rise time is calculated as the difference between the designed system signal and the Sphygmocor signal.

Second Systolic Peak

The second systolic peak is due to the reflection caused by a change in the artery's impedance [21, 22]. Assessment of the wave reflection is useful in determining the Augmentation index, pulse wave velocity and arterial stiffness [1]. It is important that the second peak is not distorted in any way as this would provide an incorrect assessment for the patient.

The error in time and pressure is calculated as the difference between the designed system and the Sphygmocor system.

Dicrotic Notch

The dicrotic notch, as shown in Figure 4.6 is also used as a measured for arterial diseases when analysed together with the second systolic peak [4, 21]. Once again, the dicrotic notch cannot be distorted by the measuring system.

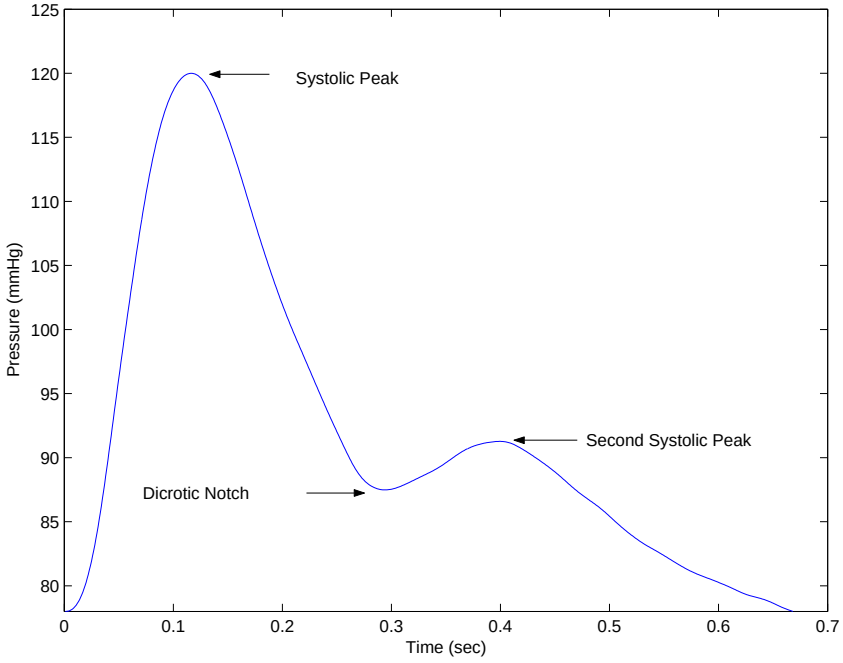


Figure 4.6: Parameters for comparison of the wave shapes

The error in pressure and time is calculated in the same way as the second systolic peak.

Root-Mean-Square Error

The RMS error is calculated using Equation 4.3, where *Predicted* is the designed system data and *Actual* is the Sphygmocor data.

4.5.3 Frequency Analysis

Fast Fourier Transform

An analysis of the frequency spectrum was performed to determine the frequency harmonics of both systems. The analysis was performed by applying a Fast Fourier Transform (FFT) to both systems. The FFT algorithm used a 32768 point Discreet Fourier transform (DFT) algorithm with a Hanning Window.

The frequency response analysis provided information about the main frequency components as well as a measure of how much the signal is distorted by the measurement system [38].

The frequency harmonics were analysed by comparing the normalised FFT of both systems [38]. A normalised FFT was used since only the ratio of the frequency harmonics was being investigated so the actual value was of little importance. An example of the FFT of both systems can be seen in Figure 4.7 (a–c). The FFT of the designed system and the Sphygmocor system are shown in Figures 4.7 (a) and (b) respectively. The comparison of the FFT for both systems is shown in Figure 4.7 (c). The results of the FFT for all the test subjects can be found in Appendix C.4.

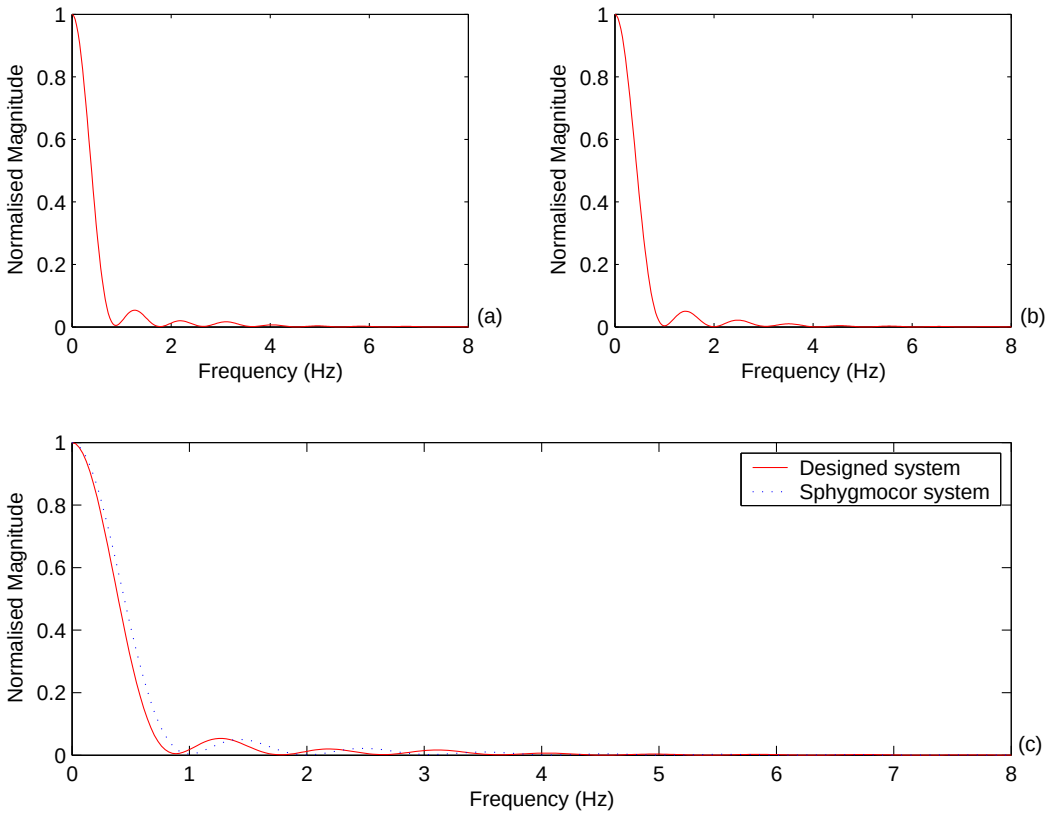


Figure 4.7: Example of the comparison of the frequency spectrum. (a) Frequency spectrum of the designed system; (b) Frequency spectrum of the Sphygmocor system; (c) Comparison of the frequency spectrum between two systems

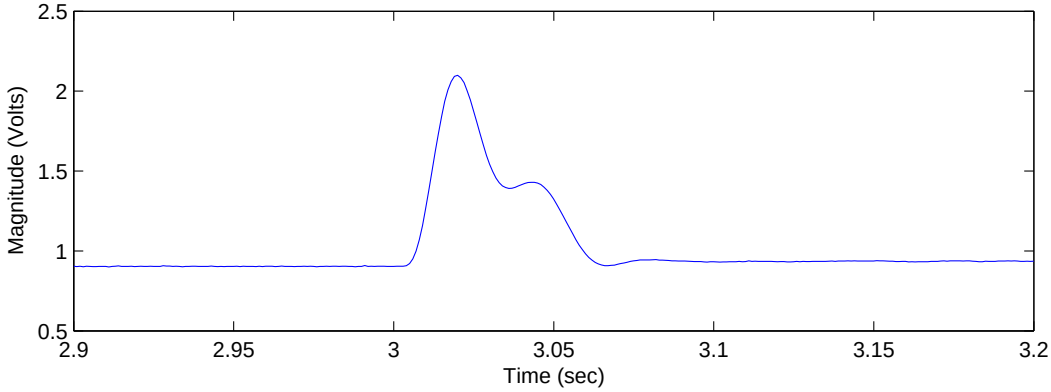


Figure 4.8: Impulse response of the designed system.

Impulse Response of the Designed System

A model of the designed system was calculated by estimating a Laplace transfer function ($H(s)$). The transfer function was calculated using convolution of the impulse response [38]. A simple test was set up to simulate an impulse, and measure the response.

In the impulse response set-up the pressure transducer was placed on a solid surface and held firmly. A short, sharp strike to the transducer with a pen simulated an impulse. The impulse response was measured at the output of the Butterworth filter (Output 1 of Figure 3.1 on Page 36). Figure 4.8 shows the recorded impulse response. This test set up only worked for the designed system. Unfortunately due to limitations in hardware and software an impulse could not be recorded from the Sphygmocor system. Analysis and discussion of the impulse is presented in Chapter 5.

Chapter 5

Test Results

5.1 Overview

This chapter presents the results of the comparisons and tests as described in Chapter 4. The measurement procedures of the two systems are compared and discussed. The results of the testing methods outlined in the previous chapter are presented. This includes determining the foot of the pulse, assessment of the pulse signal, comparison of the two systems and an assessment of the frequency spectrum. The analysis of the impulse response is included in an effort to model the transfer function of the designed system.

5.2 Comparison of Testing Procedures

The procedure to record the pulse wave using the designed system was more complicated than the Sphygmocor system. During testing, the pulse wave shape was retrieved easily and quickly, and with better quality using the Sphygmocor system than the pulse retrieved from the designed system. This was ascribed to several factors.

- The size of the pressure transducer. The smaller pressure transducer of the Sphygmocor system made it easier to find the pulse. The pulse was difficult to measure using the larger transducer particularly in the case of the female tests subjects with small wrists.

- Physical design of the pressure transducer. The Sphygmocor incorporates a pen like transducer. This was easy to hold and keep steady while recording the pulse. The designed system's transducer was in a small rectangular box which was clumsy and difficult to hold.

- The operator / physician. A steady hand was required to measure the pulse accurately and acquire a good quality signal. The Sphygmocor operator has been trained to identify and measure the pulse wave using the Sphygmocor system, and she has extensive experience in PWA. This experience, and having a steady hand has led to her recording good quality signals. The operator of the designed system could not always retrieve a good quality signal due to the lack of experience in identifying and measuring the pressure pulse. This inexperience also made it difficult to keep the transducer steady.

- As previously mentioned, two different operators, with different levels of experience, were used for the different systems. This inconsistency resulted in the high variability of the results measured from the designed system.

- The Sphygmocor incorporated some filtering and preprocessing into the system which assists with pulse identification. The lack of filtering in software for the designed system meant that the pulse signal was not always clearly identified.

These problems did not prevent the pulse from being recorded properly. Although there were difficulties in measuring the pulse using the designed system,

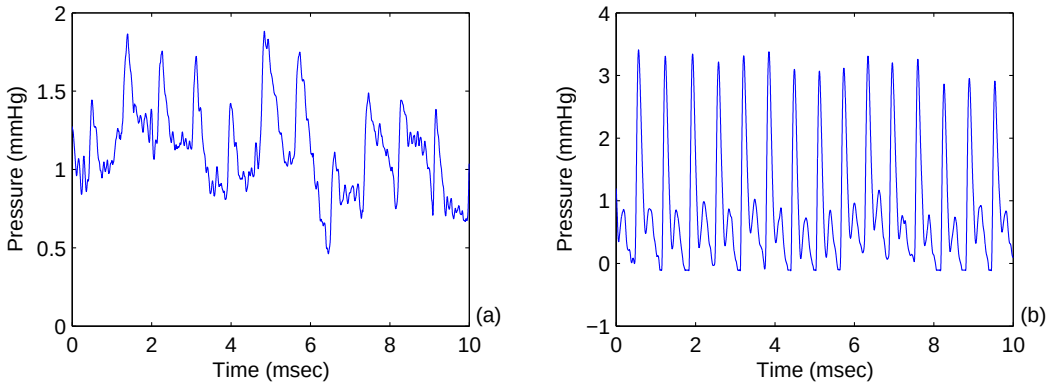


Figure 5.1: Comparison of pulse quality. (a) Poor quality pulse; (b) Good quality pulse

good quality, ten second pulse trains were recorded in three of the tests subjects. For the remaining test subjects only a portion of the full ten second recordings were used for further analysis. A poor quality signal and a good quality signal are shown in Figure 5.1(a) and Figure 5.1(b) respectively. Time permitting, more experience in performing the measurements could be gained and more readings could be recorded properly.

Both systems did not require a large amount of applied pressure. The applied pressure was measured on the designed system and was calibrated to the curve in Figure 3.6 on page 48. The average applied pressure on the skin was measured to be 35 mmHg. Patients reported no discomfort from either system during and after the tests. Neither of the pressure transducers left any visible pressure marks on the skin.

5.3 Results of Pulse Foot Identification

The pulse train was separated into individual pulses using three different methods. These methods are described in detail in Section 4.4. The different methods were compared using the diagnostic measurements: Time difference (τ), Correlation Coefficient (CC) and Root Mean Square (RMS) error, which have

Measure	Designed system		
	Method 1	**Method 2**	**Method 3**
CC	0.90± 0.05	0.90± 0.09	0.86 ± 0.16
RMS Error (mmHg)	7.5± 6.02	11.3± 6.02	18.0± 16.0
τ (msec)	-5.36 ± 22.0	-0.86 ± 17.5	-0.67 ± 14.6
	Sphygmocor		
	Method 1	**Method 2**	
CC	0.99 ± 0.006	0.99 ± 0.005	
RMS Error (mmHg)	3.11 ± 3.60	3.80 ± 4.41	
τ (msec)	-2.30 ± 5.23	-1.91 ± 5.38	

The ECG algorithm (Method 3) was not applied to the Sphygmocor data.

Table 5.1: Results of methods to identify the foot of the pulse

been described in Section 4.4. The diagnostic measurements are represented as Mean ± Standard Deviation. Table 5.1 provides a summary of the results from the three different methods. The pulses retrieved from each method are shown in Figure 5.2 (a–c) and a comparison can be seen in Figure 5.2 (d). The full set of results can be found in Appendix C.2.

The location of the pulse foot was the most consistent when using the Second derivative method (Method 2). All the pulse signals were prepared for further analysis by separating the pulse using Method 2.

5.4 Quality of Pulse Wave Shape

The quality of each pulse signal was compared and the overall results are summarised in Table 5.2, which are expressed as mean ± SD. The distribution of the results are shown Figure 5.3(a–d).

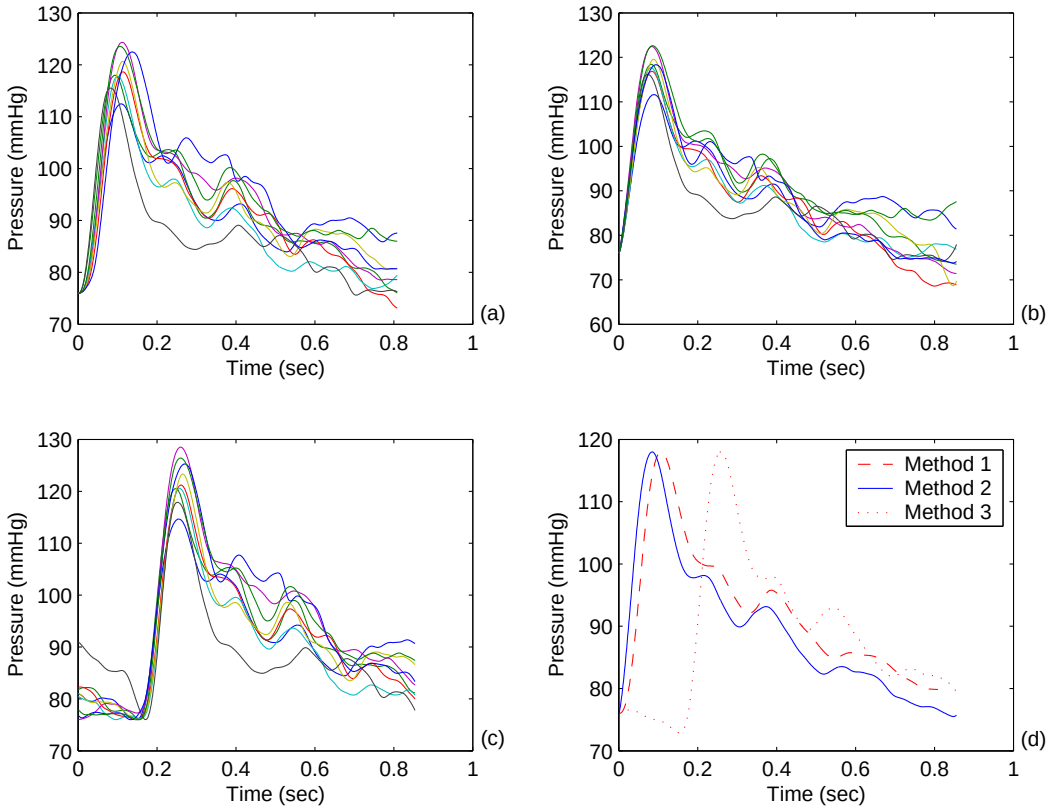


Figure 5.2: Results from the different methods of calculating the foot of the pulse. (a) Method 1 result; (b) Method 2 result; (c) Method 3 result; (d) comparison of the mean pulses of the three methods.

Diagnostic Measure	**Designed System**	**Sphygmocor System**
Error in Systolic Pressure (mmHg)	2.3 ± 18.9	0.10 ± 6.67
Percentage Error in Systolic Pressure (% mmHg)	1.3 ± 8.3	0.07 ± 3.36
Error, Pressure Rise Time (τ) (msec)	-0.87 ± 17.5	-1.92 ± 5.4
Correlation Coefficient	0.90 ± 0.09	0.99 ± 0.01
RMS error (mmHg) (RMS_{std})	11.35 ± 18.9	3.80 ± 4.41

Table 5.2: Assessment of quality of pulse wave recording

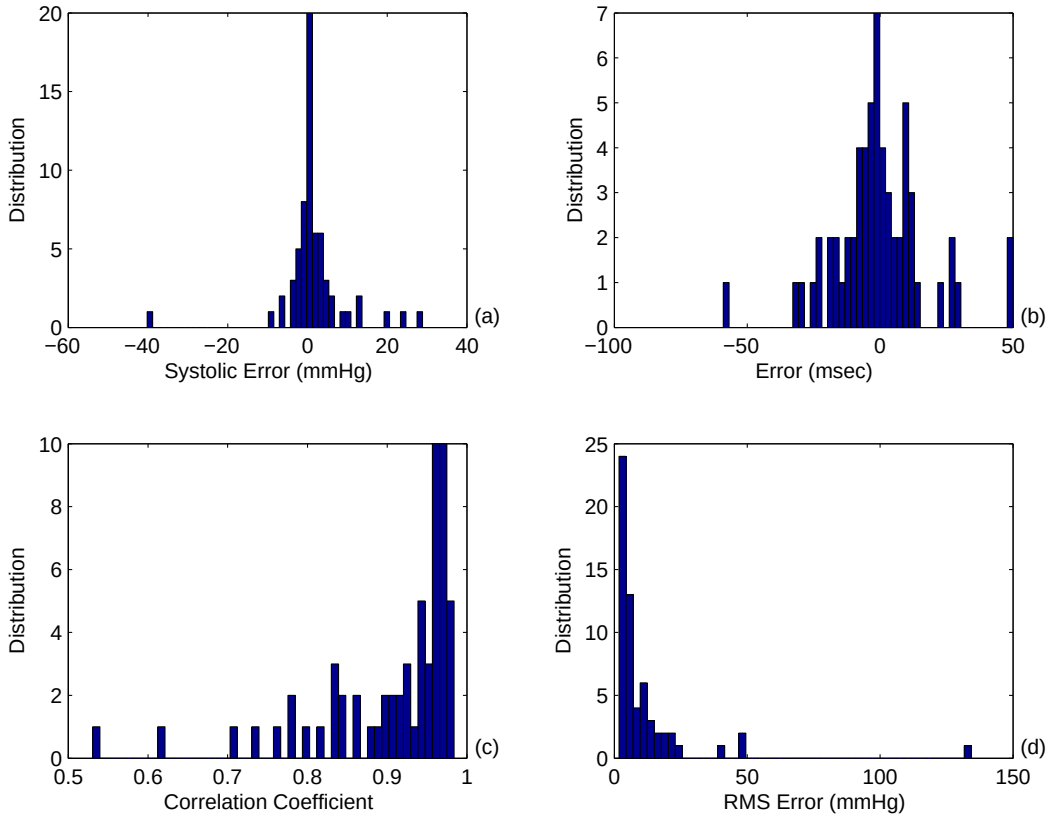


Figure 5.3: Results of quality assessment (a) error in Systolic peak; (b) error in systolic rise time; (c) correlation coefficient; (d) RMS error of individual pulses (RMS_{std})

The quality assessment of the pulse wave shape revealed that the errors in the Designed system were approximately three times higher than the errors of the Sphygmocor system. The Standard deviation was very high in comparison, which can be attributed to the signal fluctuations caused by poor measurements. In the case of the systolic pressure, the error was much greater for the designed system. This is seen by the error (2.3 ± 18.9 mmHg). In the distribution shown in Figure 5.3(a) Systolic errors can be seen at extreme values of −40% and 30%. These extreme values contribute to the high standard deviation. The rise time of the systolic peak proved to be consistent, with an error of −0.87 ± 17.5 ms. This was better than the rise time of the Sphygmocor system. These two measurements show that although the pulse varied in height, the foot of the pulse was always measured accurately.

The variability of the pulse signal is measured by the RMS Error (RMS_{std}) of the signal and can be seen in Figure 5.3(d). The average RMS error of 11.35 ± 18.9 mmHg is much greater than that of the Sphygmocor data (3.81 ± 4.41 mmHg). Part of this high average is attributed to a poor pulse recording from subject 8 (RMS_{std} = 134 mmHg). If the results from subject 8 were omitted the RMS Error would be reduced to 6.92 ± 5.38 mmHg, which would be more acceptable. Although the designed system showed a high variability, the correlation coefficient was high (0.90 ± 0.09). The pressure pulse of test subject 8 was difficult to record and as a result a poor pulse signal was captured. Even with this large variation of subject 8, all of the test subjects results were used for the comparison against the Sphygmocor.

5.5 Comparisons Against Sphygmocor

The results of the comparison are summarised in table 5.3, and are represented as mean ± SD. Figure 5.4(a–f) shows the distribution of the pressure and time

for the first and second systolic peak and the dicrotic notch. The distribution of the RMS error is shown in Figure 5.4(g). The errors shown in Figure 5.4(b–f) are the errors between the mean pulse measured from the designed system and the mean pulse measured from the Sphygmocor system. Since the mean pulse from both systems was calibrated to the systolic pressure measured from the sphygmomanometer, the error in systolic pressure between the mean pulses would be zero. Therefore Figure 5.4(a) shows the error between the individual pulses, for each subject, from the designed system with the mean pulse measured from the Sphygmocor system.

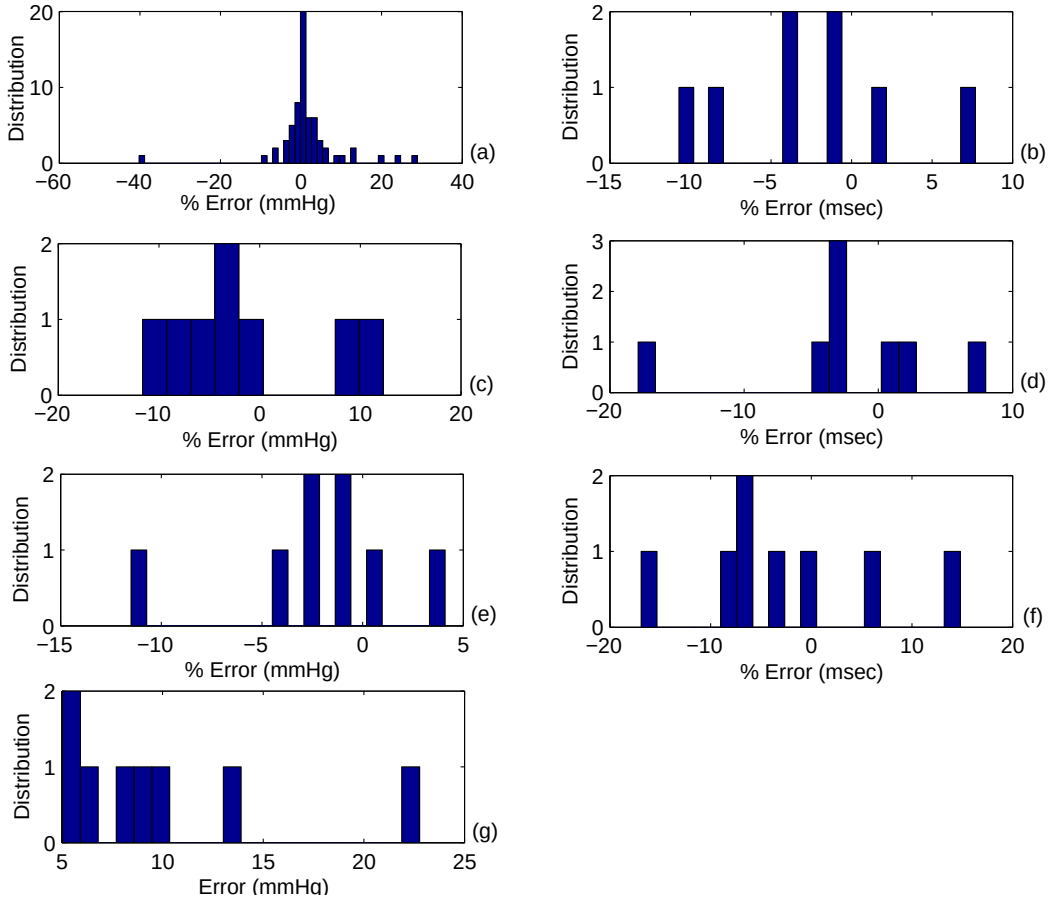


Figure 5.4: Results of comparison measurements: Percentage error of systolic pressure (a) and time (b); Percentage error of dicrotic notch pressure (c) and time (b); Percentage error of second systolic pressure (e) and time (f); (g) distribution of RMS error

The pressure pulse measured from the designed system had a decrease in pressure at the dicrotic notch (-1.1 ± 8.57 mmHg) and at the second systolic peak

Diagnostic Measurement	**Pressure (mmHg)**		**Time (msec)**	
	Error	**% Error**	**Error**	**% Error**
Systolic Peak	2.3 ± 18.9	1.3 ± 8.3	-1.9 ± 5.3	-2.4 ± 5.6
Dicrotic Notch	-1.1 ± 8.57	-1.6 ± 8.1	-2.3 ± 13.8	-2.4 ± 7.4
2nd Systolic Peak	-2.3 ± 4.4	-2.3 ± 4.5	-8.1 ± 36.2	-2.3 ± 9.7
RMS Error (mmHg)	9.99 ± 5.83			

Table 5.3: Results of Sphygmocor comparison

(-2.3 ± 4.4 mmHg). In six of the test subjects the time to the dicrotic notch and second systolic peak was shorter when measured with the designed system. This can be seen in the systolic peak of the pulse shown in Figure 5.5. The percentage errors for the time to the dicrotic notch (-2.4 ± 7.34 %) and the second systolic peak (-2.3 ± 9.7 %) are similar. This constant error in time can either be attributed to a change in pulse rate or a delay in the Sphygmocor system. Although a change in pulse rate is not impossible, every subject's pulse rate would of needed to increase to provide the calculated time error. It can be seen in Figure 5.5 that the waveform of the designed system exibits a quicker decrease in pressure after the systolic peak in comparison to the Sphygmocor waveform. As previously mentioned, the Sphygmocor systems incorporates an algorithm to determine the transfer function of the arterial system. This algorithm could create this small delay which is noticable in Figure 5.5.

The average systolic peak is greater in the designed system (2.3 ± 18.9 mmHg), however, the distribution of the error shows the error evenly distributed around zero. Since the system is calibrated to the blood pressure measured from the sphygmomanometer, this difference can be attributed to the quality of the pulse signal and not to distortion of the pulse by the measuring system.

Overall the pulse wave shape measured with the designed system was an accurate representation of the Sphygmocor system. There was a time difference

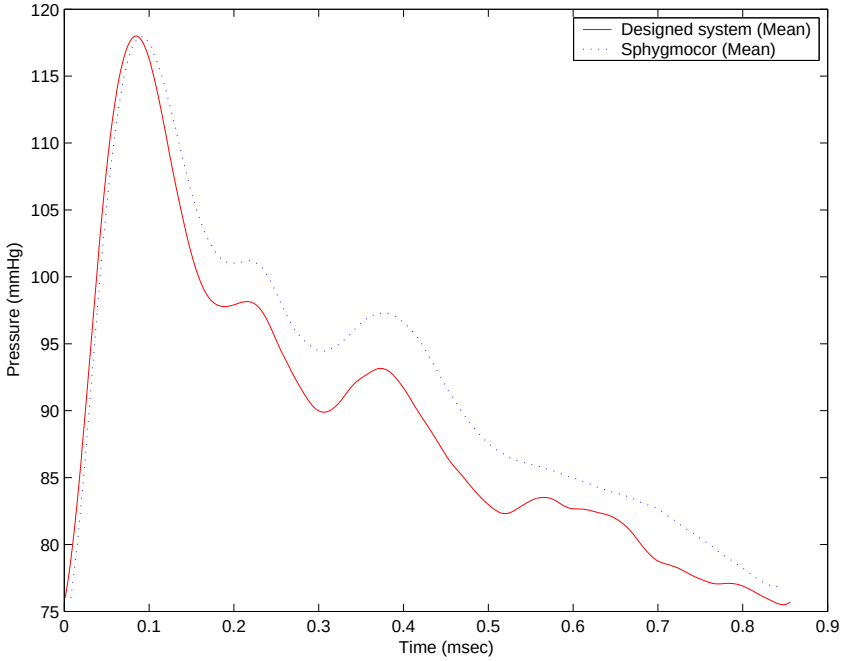


Figure 5.5: Comparison of the pulse between the two systems

between the two measurements. This error could be confirmed, in future studies, by comparing the designed system with other invasive and non-invasive PWA systems. Since the Sphygmocor could not be guaranteed as a true reflection of the pulse, it cannot be said for certain whether the error was caused by the designed system or the Sphygmocor system. This would need to be confirmed by analysing a transfer function of the designed system.

5.6 Frequency Analysis

5.6.1 Frequency Spectrum

The frequency spectrum of the arterial systems, which was presented in Chapter 4 has the majority of the power dispersed below 5 Hz. The main frequency harmonics of the arterial pulse, measured from both systems were located near DC, 2 Hz, 3.5 Hz and 4 Hz. These harmonics fluctuated slightly between the different test subjects, but the fluctuation was consistent in both systems.

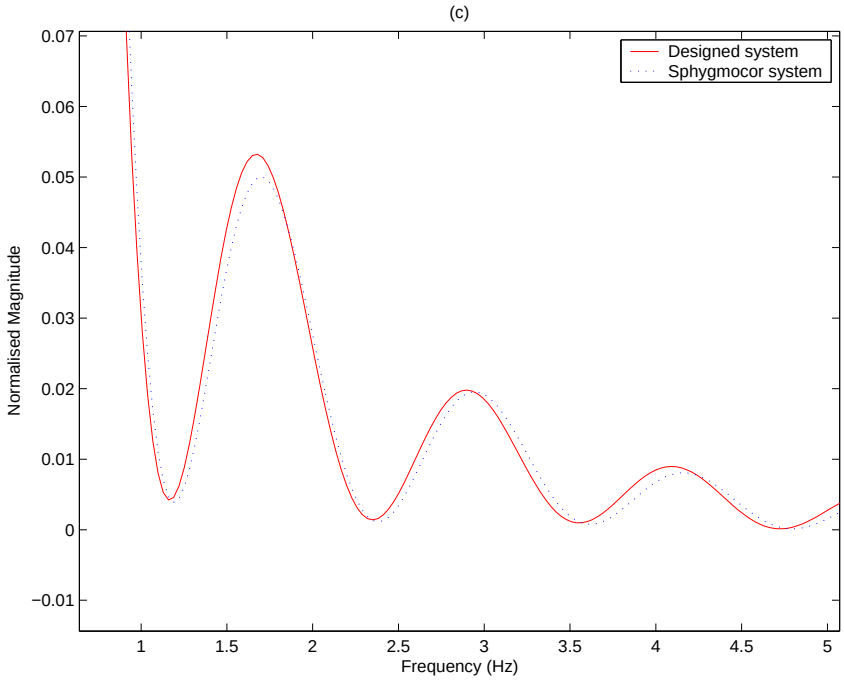


Figure 5.6: Magnified section of the frequency spectrum

The pulses measured from the designed system did not contain any additional frequency components even though the sampling frequency of the designed system was higher than that of the Sphygmocor.

The comparison of the normalised FFTs between the two systems revealed that the ratio of power between the first harmonic and subsequent harmonics are equal for both systems. This can be seen in the magnified frequency spectrum shown in Figure 5.6. The did appear do be a small frequency shift in some of the results, however this could be attributed to rounding errors.

5.6.2 Impulse Response

The impulse response was used to calculate the transfer function of the overall system. The transfer function $H(S)$ is defined as the output $(Y(S))$ divided by the input $(X(S))$ in the frequency domain; $H(S) = \frac{Y(S)}{X(S)}$. For an impulse, $X(S)$ equals 1 [38]. Therefore the transfer function of the designed system

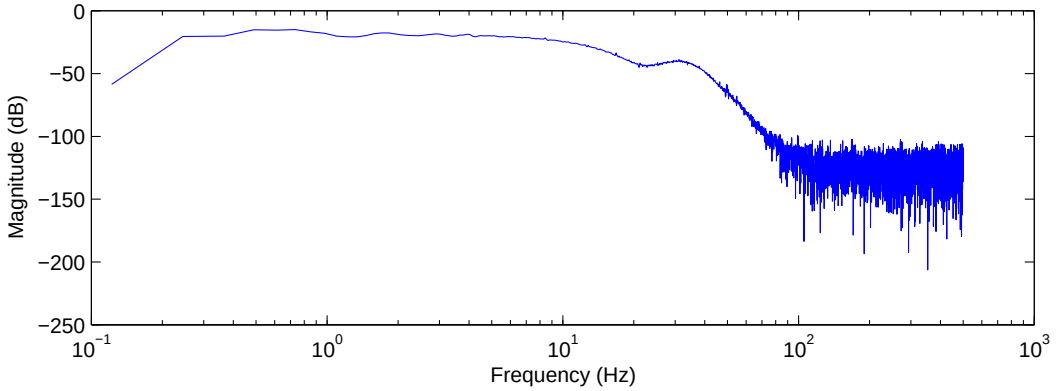


Figure 5.7: Transfer function of the designed system

was calculated by applying the FFT to the impulse response ($y(t)$) (Shown in Figure 4.8).

The transfer function, which can be seen in Figure 5.7, clearly shows the expected roll-off at 40Hz (due to the Butterworth LPF) and the roll-off before 0.3Hz (due to the High-Pass filter). Imperfections in the pass-band, and an additional roll-off at 10Hz are also present. These are possibly the result of a non ideal test set-up, the non linearities present in the pressure sensor, or the error in capacitance due to the capacitors used in the Butterworth filter. Higher frequency components ($>$ 70Hz) were attenuated to between -150 and -200 dB as expected.

Chapter 6

Conclusion

6.1 Discussion

Hardware

The arterial tonometry system designed for this research was able to measure and record the arterial pressure pulse. The signals recorded contained large fluctuations and DC drift, which was due to flaws in the hardware design, particularly the pressure probe. These large fluctuations resulted in the signal being separated into individual pulses and only being able to compare the average pulse of the signal.

The main focus on the hardware design was electrical safety. The system was required to meet the IEC 601 safety standard. This ensured the patient's safety by isolating the system from any high voltages and breaking the ground connection between the patient and high voltage equipment. The designed system was based upon a battery power supply and incorporated electrical isolation. Electrical safety was tested with the use of an IEC 601 testing station, which tested leakage current and patient auxiliary current. The overall

results revealed that the system fell well within the safety limits and was acceptable for use on humans.

The hardware design was based on a low voltage single supply 5 Volt system. All the components were chosen for their accuracy and precision. The design did not make use of any components which were expensive or difficult to obtain. The total component cost of the system amounted to less than R2000. Should this design be taken further, the designer would not have any problems in sourcing components.

The primary concern in the design was the pressure transducer. This, along with the lack of experience of the operator (for the designed system), were the main factors for recording poor signals. The transducer was too large for the required application. In any further design a sensor with similar characteristics but a smaller pressure diaphragm should be used. The design of the housing for the sensor requires a lot more thought. A smaller, less clumsy housing, which is easy to hold would be better suited for blood pressure measurements. An experienced operator would be able to find the best pressure pulse and be able to keep the transducer steady. This will result in the best quality signal being recorded.

In this research the signal was sampled at 1kHz, where the Sphygmocor system only sampled at 128Hz. The larger sampling frequency was chosen in an attempt to find any other frequency components which may have been lost by the lower sampling frequency of the Sphygmocor. A FFT of the signals from both systems revealed that no extra frequency harmonics existed and that the majority of the power was below 10Hz. These findings correspond to the research by Fetics [36] and O'Rourke [19].

Data Analysis

The signal was analysed by assessing the variability of the pulse (quality of the pulse) and by comparing the average pulse wave shape measured from both systems. The pulse variability yielded a standard deviation (RMS Error) of 11.35 $\pm$ 18.9 mmHg, with a systolic pressure error of 2.3 $\pm$ 19.9 mmHg. The cause of this error is attributed to the large clumsy sensor and operator inexperience. In a larger group of test subjects and with more measurement experience the RMS error could be reduced.

The pulse wave measured from the designed system contained the same components and followed the same contour as that of the Sphygmocor system and no data was lost from the pulse contour. The measurements from the designed system showed errors in the time difference (-2.4 ± 7.34 %) and in pressure (-1.1 ± 8.57 mmHg). The source of the error has been attributted to difficiencies in the hardware design and inconsiatancies in the measurement procedure.

The transfer function ($H(s)$) of the designed system was estimated in an attempt to model the system. An analysis of the transfer function showed the expected roll-off at the 0.3Hz and 40Hz, however the pass band was not very flat.

6.2 Further Research

The scope of this research did not cover every aspect of pulse wave analysis. This research could be extended to cover the following topics:

Comparison with Invasive Arterial Measurements

Invasive measurements of the arterial pulse wave shape would provide the most accurate data. Problems such as sensor position, DC drift and the reliability of a steady hand to record the pressure would be eliminated. A comparison between a direct arterial pressure measurements and non-invasive measurements using the designed system would be required to identify the extent of signal distortion caused by the designed system.

Aortic transfer function

Extensive research has been conducted in estimating the transfer function between the aortic pulse and the radial pulse. O'Rourke [1, 19] has developed a transfer function which is used in the Sphygmocor system. Other research conducted by Millasseau et al [10], Segers et al [13] and Fetics et al [36] have assessed the validity of the transfer function by estimating their own transfer function and comparing the two.

Further research would involve performing intra-arterial pressure measurements in a catheter laboratory. This could be used in the estimation of an aortic transfer function and as a reference for a non-invasive pulse wave shape comparison.

Hardware improvements

The designed measurement system produced accurate results in comparison to the Sphygmocor system, however, it can be further improved. The pressure sensor was the primary factor for inaccuracies and can be improved. The sensor housing could be re-designed to be more comfortable to use. This would result in improved readings, and greater accuracies in the pulse wave measurements.

Once the hardware has been improved and finalised the viability of marketing the system can be assessed.

6.3 Conclusion

Pulse wave analysis provides valuable information in the assessment of arterial diseases. Measurements such as Augmentation index (AiX), wave reflection and pulse wave velocity (PWV) relate to the health of the arteries and the heart. To provide an accurate assessment of the condition of the arteries the pulse wave shape needs to be carefully measured. Existing systems such as the Sphygmocor PWA system provide accurate assessment of the arteries by determining the AiX, and PWV. A system was designed to investigate the design issues in a pulse wave analysis system. The system was tested and validated with data from the Sphygmocor system.

The design of the system took the necessary precautions such as patient safety and comfort into account. This was achieved through electrical isolation and by maintaining a battery power supply. The system conformed to the required IEC-601 safety standard, which ensured patient safety throughout the testing procedure.

The hardware designed consisted of signal amplification and filtering circuitry. The pulse signal was amplified from a small voltage of < 10mV to a range of 1–5V. The signal was modulated to a small degree, which was caused by the response of the filters. This modulation did not introduce any large error and the analysis was still successful. The system could be improved by a redesign of the hardware, especially the pressure probe.

The data from the two systems were compared in both the time domain and the frequency domain. In the time domain the error between the two systems was

small and was considered acceptable. The frequency spectrum revealed that the two systems produced the same harmonics and no additional information was gained or lost from either system.

The performance of the design suggests that, in some respects, the design was comparable to the commercial system, however, a number of performance characteristics fell short of the commercial system. This leaves several options for further research. The pressure probe should be redesigned for easier recordings. Research into the transfer function of the arterial system could follow on from this research, however an improved hardware design is required first.

Appendix A

Pulse Wave Analysis History

Sphygmography, the study of the arterial pulse, was started over 100 years ago. William Bright identified high blood pressure as the hardness of the pulse in his research in 1827. Frederick Akbar Mohamed, in 1872, illustrated the importance of the arterial pulse wave shape with the use of graphical methods [1, 19]. Mohamed established the foundation for pulse wave analysis as well as developing one of the first graphical methods to record the arterial pulse. He described the arterial pulse and identified the difference between the radial and carotid pulse. He also showed the effect of high blood pressure on the radial pulse

The technique to record the pulse wave was time consuming and difficult. The wave shape was also difficult to characterise and was prone to artifact. The introduction of the cuff sphygmomanometer, in the early 1900s, provided an easy solution to these problems. The cuff, which was easier to use and more accurate, produced numbers for the extreme points of the pulse. These could simply be referenced to a measure of cardiac strength. This led to the decline in interest in sphygmography [1, 19].

The study of the pulse wave shape attracted more interest and recognition with the advancement of computers and highly accurate pressure transducers.

Piezo-electric transducers, which were originally developed for intra-ocular pressure were adapted to be used for arterial purposes. These are far more accurate, reliable and easier to use than the original mechanical sphygmogram developed by Mohamed [1]. This has led to a greater understanding of the arterial system and better diagnosis of arterial diseases.

The analysis of the wave shape not only revealed systolic, diastolic and mean pressures, it also provided an assessment of the wave reflection. Wave reflection changes with the different properties of the arteries, such as hardening of arteries, and is described in Section 2.2.1. MacDonald of St Bartholomew's Hospital, London (1950s) was responsible for explaining the difference of aortic waves and peripheral waves by explanation of wave reflection in arteries. He introduced the transfer function to characterise properties of arteries in the frequency domain. The work by Macdonald as well as J.R. Womersley and Taylor, also from St Bartholomew's Hospital, has led to most of the techniques used for pulse wave analysis [1]

Appendix B

Hardware Circuits Description

B.1 Pressure Sensor Circuit

The design uses the IC-Sensor model 84 (IC Sensor, MSI, USA). This is a piezoresistive pressure sensor which uses laser trimmed resistors in a wheatstone bridge. The compensation resistor allows the sensor to be interchangeable to within ± 1% of the amplifier output span when used with the correct external resistors [28].

The model 84 transducer is excited by a constant current source between 1mA–1.5mA. The circuit to provide the current is shown in Figure B.1. The current source is controlled by the 1.235V reference diode and a 920Ω current set resistor (R_4) (1% tolerance). The current I_0 is defined as $I_0 = (E_0 - e_0)/R_4$, where E_0 is the reference voltage and e_0 is is the offset of the amplifier $IC1D$ (≈ 0). This configuration provides a current source of 1.343mA.

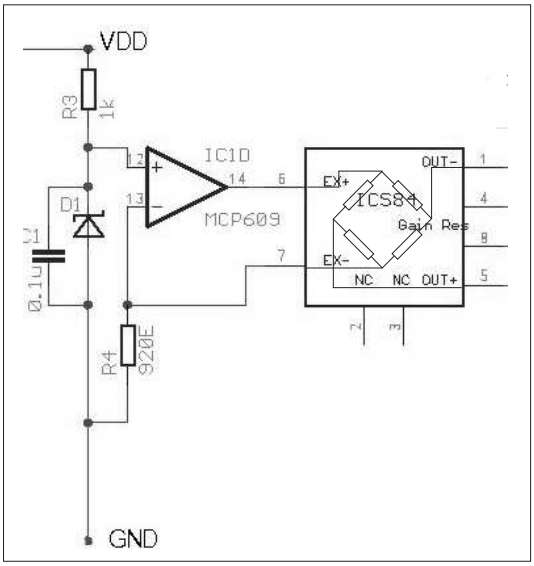


Figure B.1: Excitation circuit for the pressure sensor

B.2 Amplification Circuits

B.2.1 Pressure Amplification

The amplification for the pressure sensor was achieved using an instrumentation amplifier. The design of the amplifier, as seen in Figure B.2, used 3 op-amps instead of a single chip instrumentation amp.

The op-amps used in the circuit are Microchip MCP609 amplifiers. This is a quad packaged amplifier and its features include single supply operation, 250μV offset voltage, rail-to-rail output and a typical CMRR of 91 dB. The gain of the amplifier is controlled by the gain set resistor incorporated in the pressure sensor.

The differential input stage of the instrumentation amplifier has a gain of $Gain = 1 + (R_1 + R_2)/r$, where r is the gain set resistor of the pressure transducer. The gain set resistor r is a laser trimmed resistor calibrated to provide an output span of 2V when the excitation current is set to 0.996mA and the feedback resistors R_1 and R_2 are 100kΩ [39].

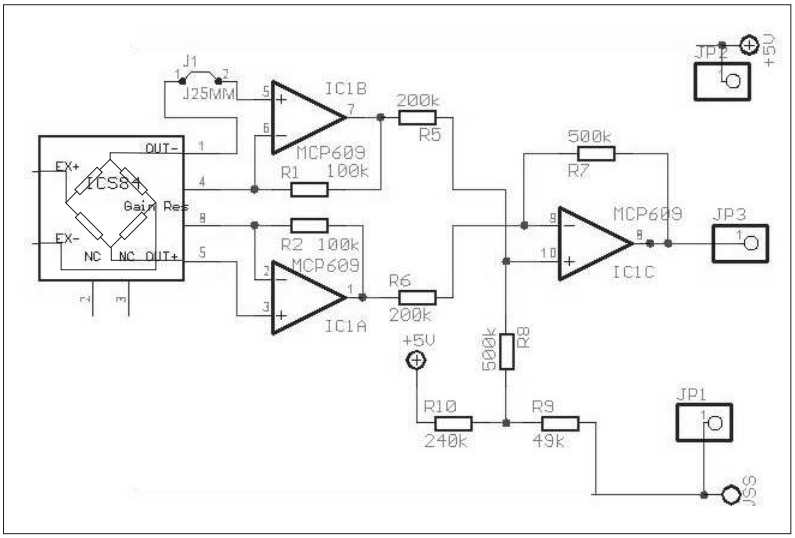


Figure B.2: Sensor amplification circuit

The instrumentation amplifier has an additional gain of R_8/R_5 resulting in the overall gain given by Equation B.1. The resistor values are set to $R_5 = R_6 = 200k\Omega$ and $R_7 = R_8 = 500k\Omega$. The ratio A is between the actual excitation current (1.343mA) and the reference current(0.996mA).

$$V_{out} = 2 \times A \times R_8/R_5 = 2 \times (1.343/0996) \times (500k/200k) = 6.74V \qquad \text{(B.1)}$$

The amplifier is supplied by 5V, therefore at full scale pressure (300mmHg) saturation will occur. Since the full scale of the pressure sensor is not used, this is not a concern.

The positive input of the differential amplifier has been biased with an additional offset of 0.85V by the voltage divide R_9 and R_{10}. This offset was introduced to overcome the forward voltage drop of the Infrared emitting diode in the optocoupler.

B.2.2 ECG Amplification Circuit

The ECG instrumentation amplifier and right leg drive circuit is shown in Figure B.3. The amplification of the instrumentation amplifier is calculated using Equation B.2 [40]. Resistor R_G is the gain set resistor $R_1 \| (R_2 + R_3) = 4.4k\Omega$. The gain of the instrumentation amplifier is calculated to be 23.2.

$$V_O = \left(1 + \frac{100k\Omega}{R_G}\right) V_C \tag{B.2}$$

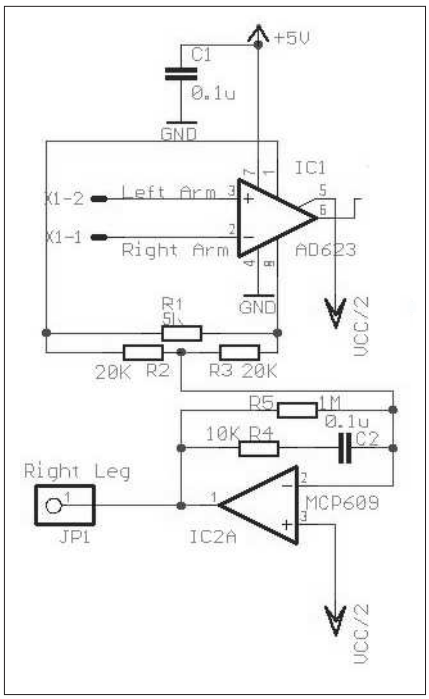


Figure B.3: ECG amplifier and right leg drive circuit

The right leg amplifies the common mode voltage at the junction of R_2 and R_3 through an inverting amplifier. The output of the amplifier is used as a reference electrode for the differential measurement. The right leg driver reduces the common mode interference of the differential inputs. Capacitor C_2 is chosen to maintain the stability of the right leg drive by reducing oscillations [22, 29].

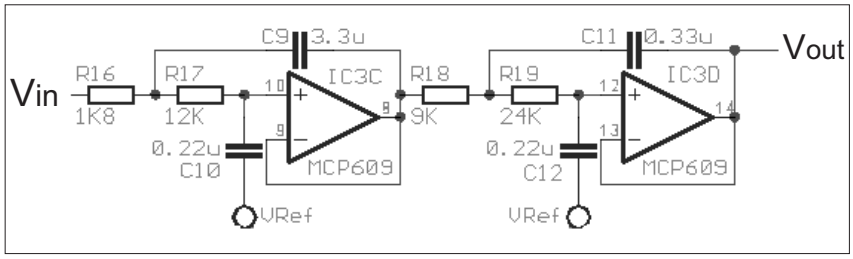


Figure B.4: Fourth order Butterworth filter used for signal conditioning

B.3 Filter Circuits

The low pass Butterworth filter as used in the arterial tonometry circuit is shown in Figure B.4. The LPF is a 4th order filter with a cutoff frequency of 40Hz and unity gain. The component values were chosen according to a sample filter design in Microchip FilterLab.

The filter, as show in figure B.5, attenuates the ECG signal to a range of 0.05–100Hz. The high pass filter is a passive filter with a unity gain and a cutoff

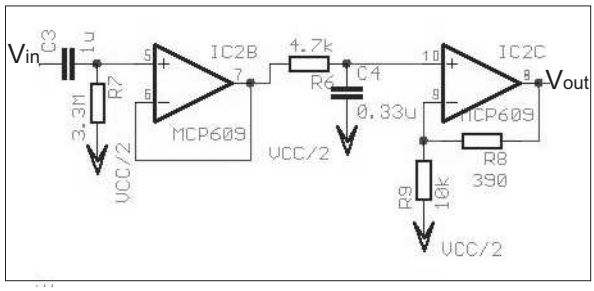


Figure B.5: First order bandpass filter

frequency of approximately 0.05Hz, as calculated in Equation B.3.

$$f_{c(hpf)} = 1/2\pi R_7 C_3 = 1/2(\pi)(3.3M\Omega)(1uF) = 0.048Hz \qquad \text{(B.3)}$$

The low pass filter has a gain of 40 with a cut off frequency of approximately 100Hz as calculated in Equation B.4.

$$f_{c(lpf)} = 1/2\pi R_6 C_4 = 1/2(\pi)(4.7k\Omega)(0.33uF) = 102.6Hz \qquad \text{(B.4)}$$

A Twin-T notch filter is used to attenuate the 50Hz line interference. The passive filter, which is shown in Figure B.6 comprises a first order high pass and first order low pass filter whose frequencies are exactly matched to the cutoff frequency of $f_c = 1/2\pi RC$. The capacitor values are all set equal; i.e. $C = C_{13} = C_{14} = C_{15} = C_{16} = 4.7nF$ and the same applies to the resistor values; i.e. $R = R_{21} = R_{22} = R_{23} = R_{24} = 680k\Omega$. By using matched values for R and C a cutoff frequency of $f_c = 49.8Hz$ is achieved. The op-amps, $IC3A$ and $IC3B$ and variable resistor R_{27} provide a tuning method to improve the notch characteristic at the notch frequency [41].

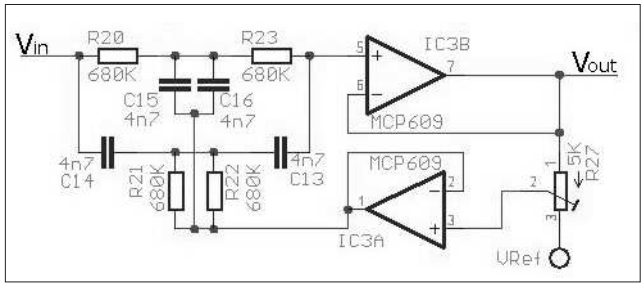


Figure B.6: Twin-T notch filter circuit diagram

B.4 Isolation Circuit

The electrical isolation circuit is shown in Figure B.7. The design uses the 4N28 optocoupler, which comprises a photo-transistor optically coupled to an infrared emitting diode. The unit is packaged in a 6-pin plastic dual-inline package. Resistor R_{10} and R_{13} limit the forward current of the emitter to below 10mA. The emitter current of the transistor is limited to below 10mA by resistors R_{14} and R_{15}.

The infrared emitting diode has a forward voltage of 1.25V [33]. In practice the forward voltage was measured to be 0.9V. In the arterial tonometry system a voltage offset of 0.85V was added to the positive pin of the Instrumentation amplifier to overcome the forward voltage. There was no need to add an offset

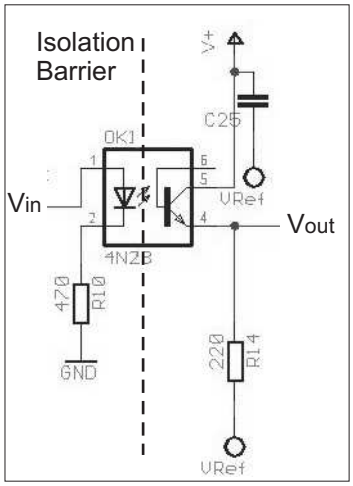


Figure B.7: Isolation circuit using an optocoupler

to the ECG circuit since the ECG signal was referenced at 2.5V. However, output voltage of the ECG amplifier had a range of 0–4.6V, referenced at 0.6V. This did not cause any loss of signal.

B.5 Circuit Diagrams

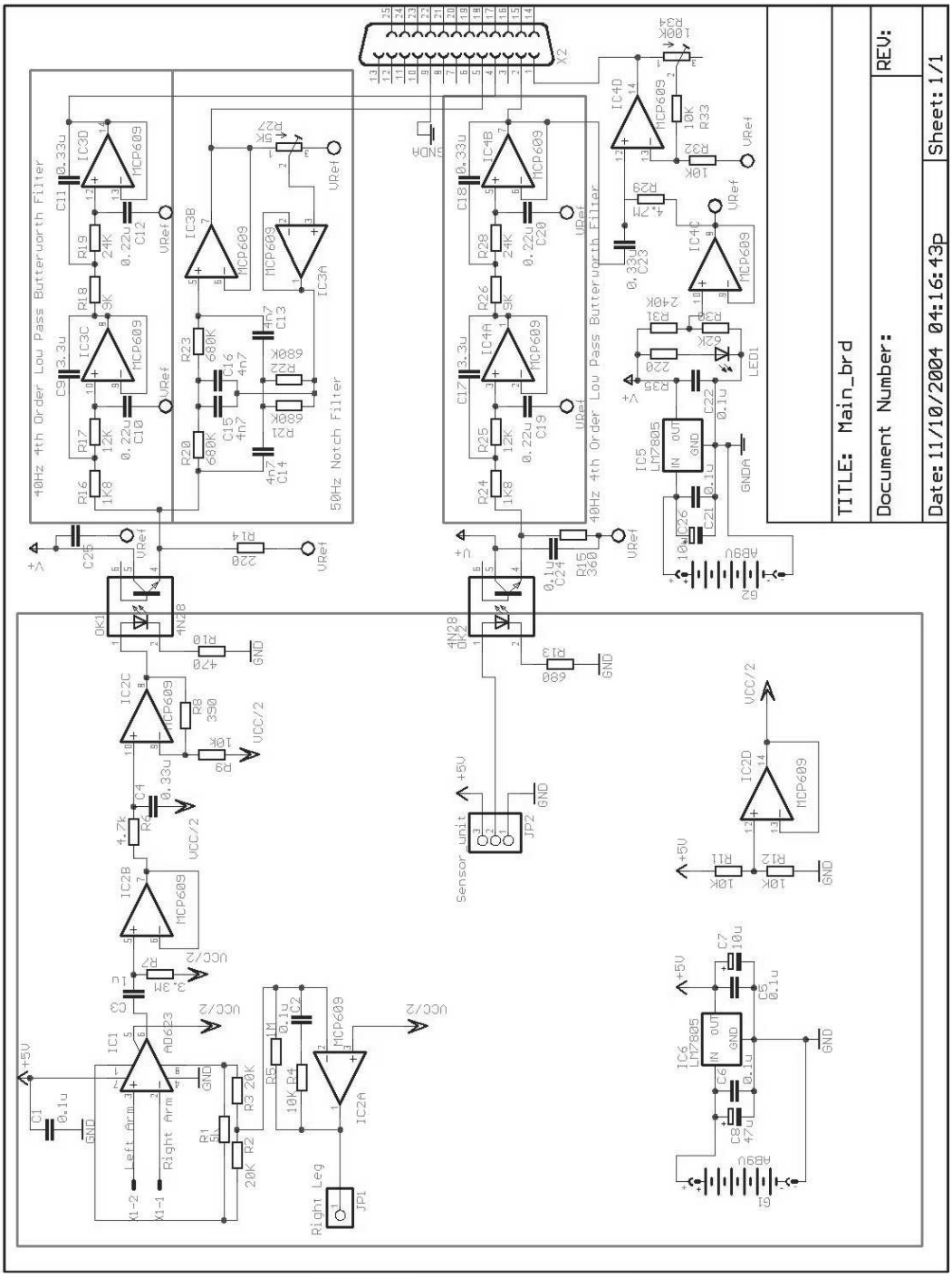


Figure B.8: Schematic of main circuit board

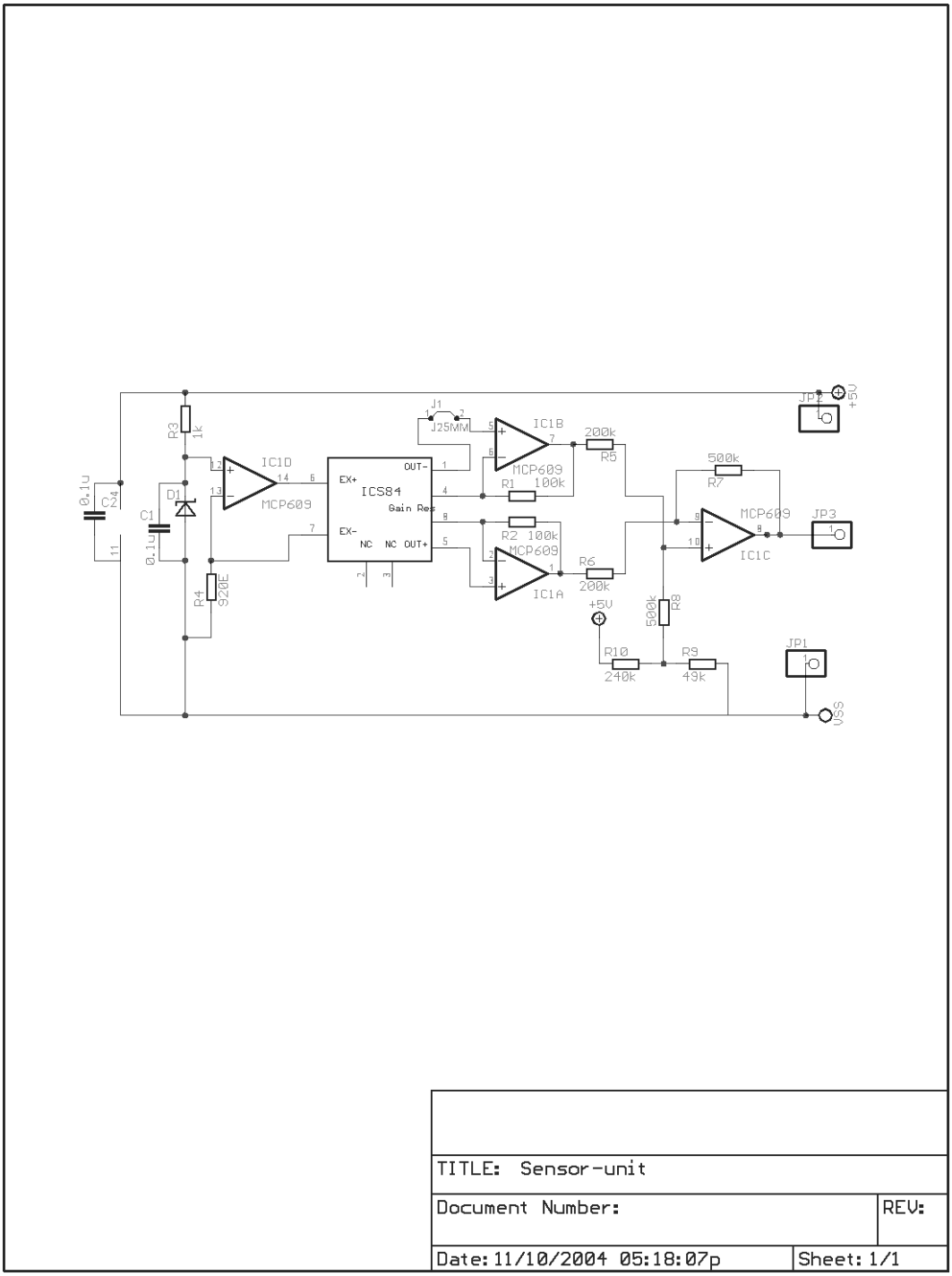


Figure B.9: Schematic of sensor unit circuit

Appendix C

Measured Data and Results

C.1 Recorded Data

The results for all test subjects are shown in Figures C.1 (a–f) to Figures C.8 (a–f). The signals measured using the designed system and the Sphygmocor system are shown in Figures C.1 – C.8(a) and (b) respectively. The pulses are separated into individual periods using the maximum second derivative method (Figures C.1 – C.8 (c & d)). The Mean ± Standard Deviation of the measured pulse from the designed system is shown in Figures C.1 – C.8(e) and a comparison of the mean pulse of both systems is shown in Figures C.1–C.8 (f).

The signals recorded using the designed system contained a lot more variation from the signals recorded using the Sphygmocor system. DC drift can be seen in the signals from both the designed system and Sphygmocor system, which was caused by movement of the pressure probe. In the case where the arterial pulse was difficult to find the quality of the recorded waveforms were poor (Figures C.1, C.6 and C.8)

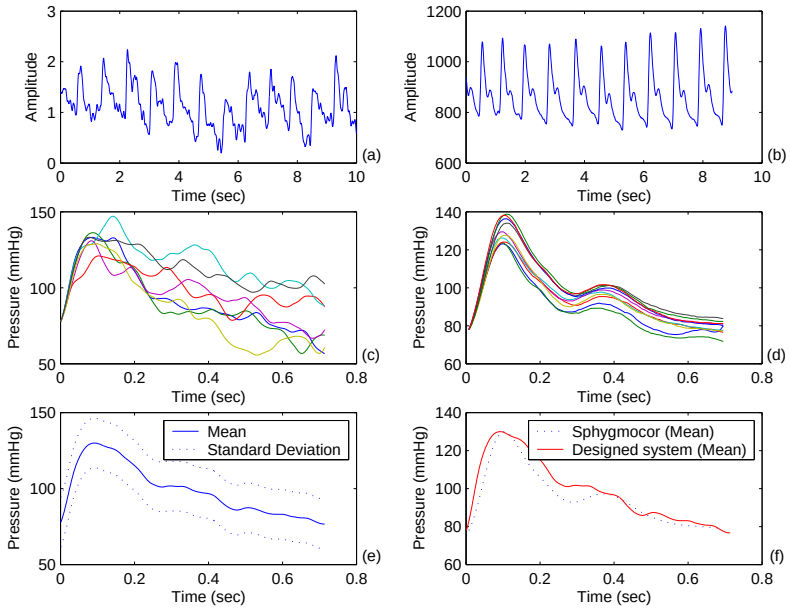


Figure C.1: Measured results of subject 1: (a) pulse signal measured using designed System; (b) pulse signal measured using Sphygmocor system; (c) separated pulse from designed system; (d) separated pulse from Sphygmocor system; (e) Mean (solid line) and standard deviation (dashed line) of pulse from designed system; (f) comparison of pulse of the designed system and the Sphygmocor system

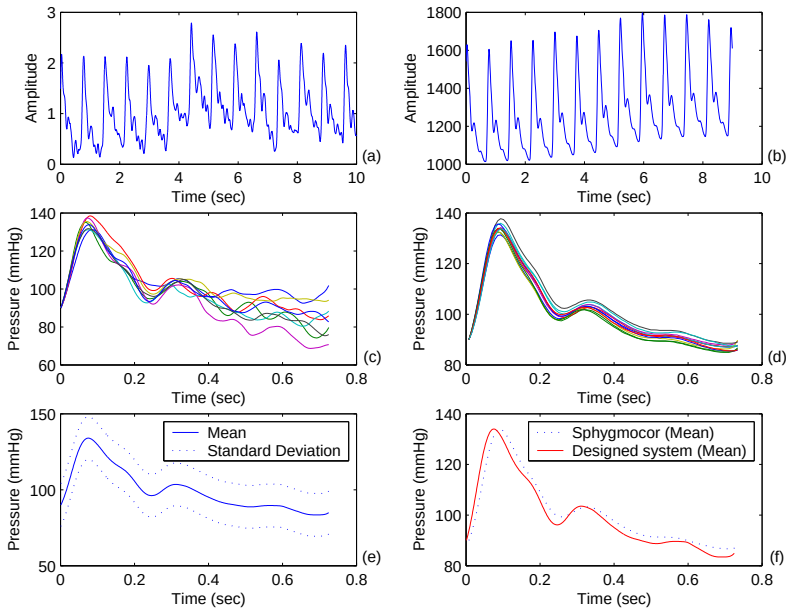


Figure C.2: Measured results of subject 3: (a) pulse signal measured using designed System; (b) pulse signal measured using Sphygmocor system; (c) separated pulse from designed system; (d) separated pulse from Sphygmocor system; (e) Mean (solid line) and standard deviation (dashed line) of pulse from designed system; (f) comparison of pulse of the designed system and the Sphygmocor system

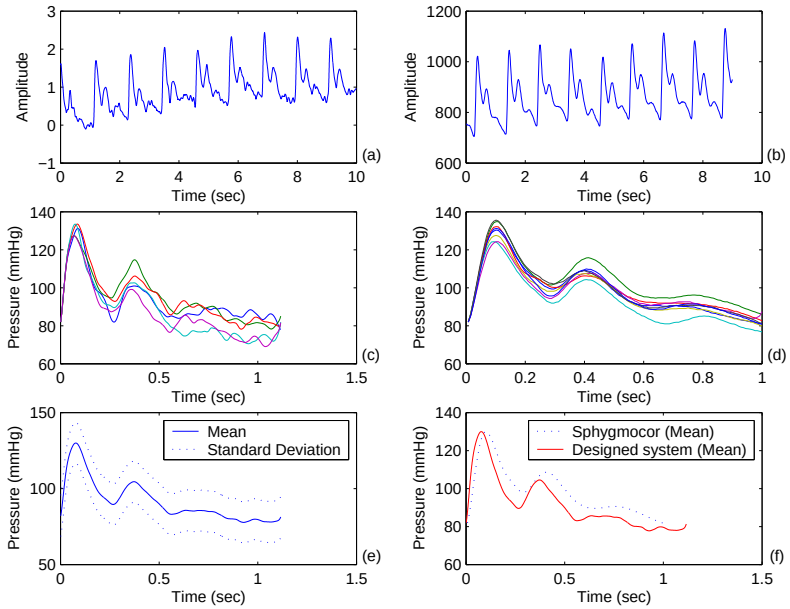


Figure C.3: Measured results of subject 4: (a) pulse signal measured using designed System; (b) pulse signal measured using Sphygmocor system; (c) separated pulse from designed system; (d) separated pulse from Sphygmocor system; (e) Mean (solid line) and standard deviation (dashed line) of pulse from designed system; (f) comparison of pulse of the designed system and the Sphygmocor system

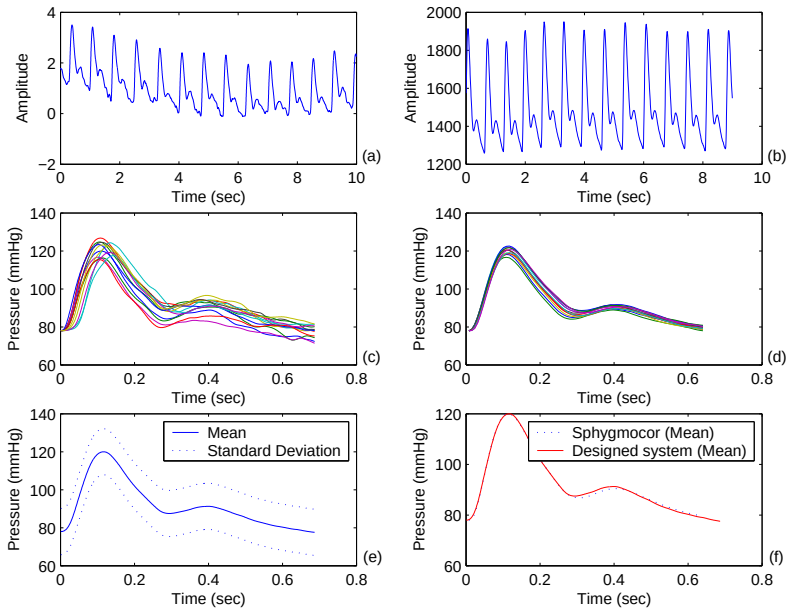


Figure C.4: Measured results of subject 5: (a) pulse signal measured using designed System; (b) pulse signal measured using Sphygmocor system; (c) separated pulse from designed system; (d) separated pulse from Sphygmocor system; (e) Mean (solid line) and standard deviation (dashed line) of pulse from designed system; (f) comparison of pulse of the designed system and the Sphygmocor system

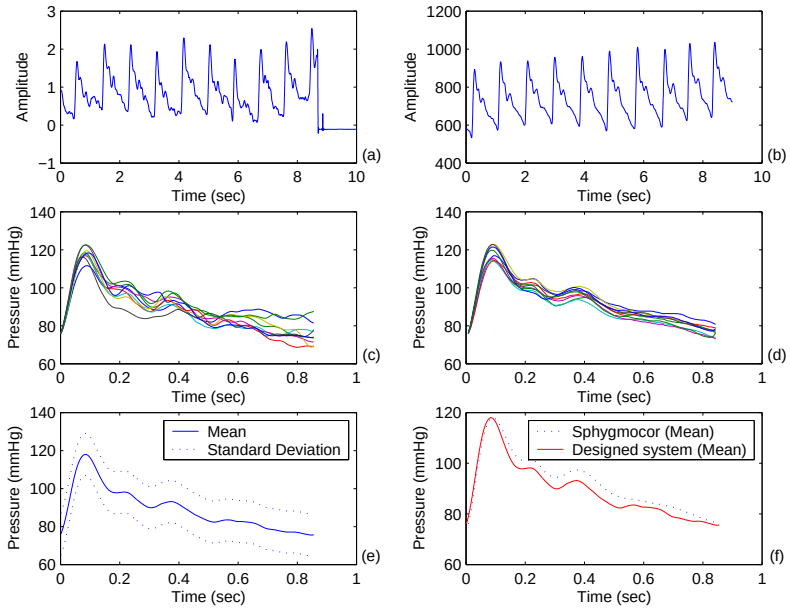


Figure C.5: Measured results of subject 6: (a) pulse signal measured using designed System; (b) pulse signal measured using Sphygmocor system; (c) separated pulse from designed system; (d) separated pulse from Sphygmocor system; (e) Mean (solid line) and standard deviation (dashed line) of pulse from designed system; (f) comparison of pulse of the designed system and the Sphygmocor system

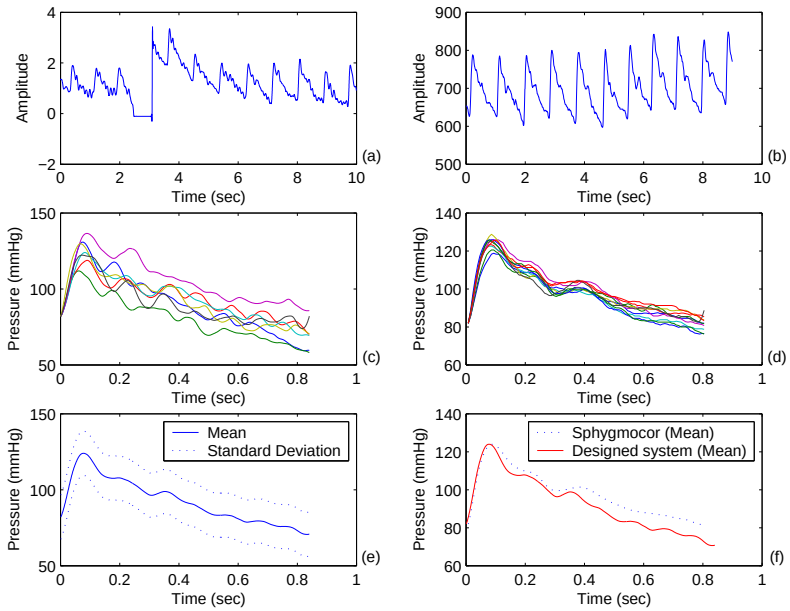


Figure C.6: Measured results of subject 7: (a) pulse signal measured using designed System; (b) pulse signal measured using Sphygmocor system; (c) separated pulse from designed system; (d) separated pulse from Sphygmocor system; (e) Mean (solid line) and standard deviation (dashed line) of pulse from designed system; (f) comparison of pulse of the designed system and the Sphygmocor system

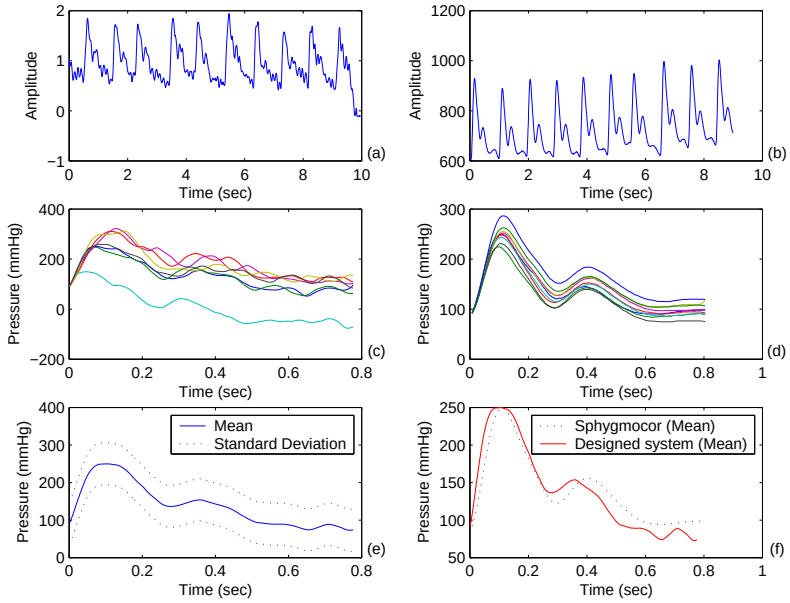


Figure C.7: Measured results of subject 8: (a) pulse signal measured using designed System; (b) pulse signal measured using Sphygmocor system; (c) separated pulse from designed system; (d) separated pulse from Sphygmocor system; (e) Mean (solid line) and standard deviation (dashed line) of pulse from designed system; (f) comparison of pulse of the designed system and the Sphygmocor system

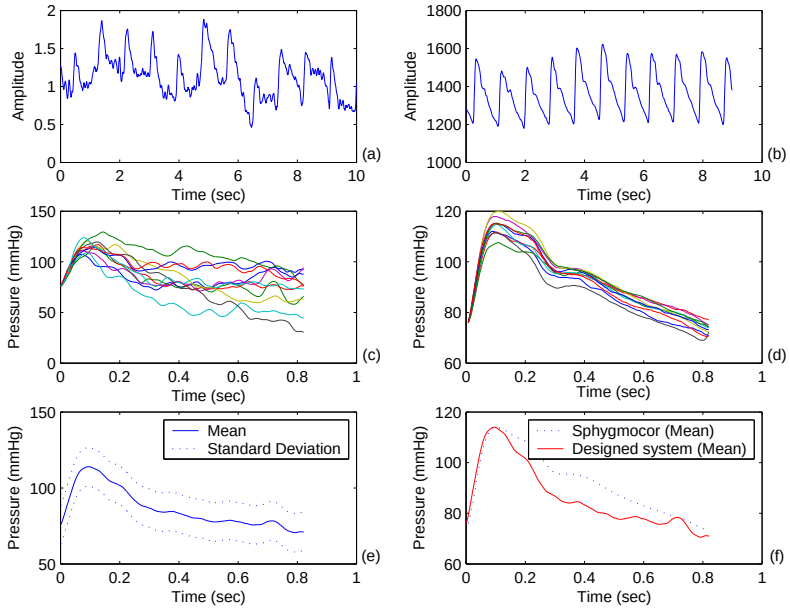


Figure C.8: Measured results of subject 9: (a) pulse signal measured using designed System; (b) pulse signal measured using Sphygmocor system; (c) separated pulse from designed system; (d) separated pulse from Sphygmocor system; (e) Mean (solid line) and standard deviation (dashed line) of pulse from designed system; (f) comparison of pulse of the designed system and the Sphygmocor system

C.2 Results of Pulse Foot Calculation

Tables C.1–C.3 present the results of the three methods used to determine the foot of the pulse wave. Table C.1 compares the correlation coefficient, Table C.2 compares the time difference of the systolic peak and Table C.3 compares the RMS Error between the individual pulses. In each table the comparison is made between the designed system and the Sphygmocor system for Methods 1 and 2. Method 3 was only applied to the designed system as no ECG was recorded for the Sphygmocor data, however, the results are still presented.

No.	**Correlation Coefficient (Mean ± S.D.)**				
	Method 1		**Method 2**		**Method 3**
	DS	SPH	DS	SPH	DS
1	0.84 ± 0.04	0.98 ± 0.004	0.87 ± 0.03	0.99 ± 0.003	0.85 ± 0.03
3	0.85 ± 0.06	0.99 ± 0.001	0.96 ± 0.01	0.99 ± 0.001	0.96 ± 0.01
4	0.92 ± 0.02	0.98 ± 0.002	0.96 ± 0.01	0.99 ± 0.002	0.96 ± 0.01
5	0.94 ± 0.02	0.99 ± 0.002	0.98 ± 0.01	NR	NR
6	0.92 ± 0.04	0.99 ± 0.004	0.95 ± 0.02	0.99 ± 0.004	0.94 ± 0.04
7	0.91 ± 0.04	0.98 ± 0.006	0.95 ± 0.01	0.98 ± 0.006	0.79 ± 0.02
8	0.94 ± 0.01	0.99 ± 0.005	0.90 ± 0.04	0.99 ± 0.004	0.93 ± 0.01
9	NR	NR	0.74 ± 0.09	0.99 ± 0.003	0.77 ± 0.06
Mean	0.90	0.99	0.90	0.99	0.86
SD	0.05	0.01	0.09	0.01	0.16

NR = No Result, DS = Designed system, SPH = Sphygmocor system

Table C.1: Comparison of correlation coefficient.

No.	Systolic Time Delay (τ)(msec) (Mean ± S.D.)				
	Method 1		Method 2		Method 3
	DS	SPH	DS	SPH	DS
1	−10 ± 31	−4.7 ± 6.6	5.2 ± 21	0.78 ± 5.76	3.0 ± 20
3	−7.6 ± 21	−0.7 ± 2.4	−0.86 ± 4.2	−2.8 ± 3.95	0.64 ± 6.23
4	0.28 ± 16.8	−4.4 ± 4.17	−0.6 ± 8.67	−1.11 ± 2.95	0.42 ± 7.56
5	−0.69 ± 13.7	−4.26 ± 4.08	−1.14 ± 7.20	NR	NR
6	5.2 ± 20.2	−0.86 ± 4.69	−0.11 ± 5.96	−4.34 ± 4.11	-0.11 ± 6.82
7	−1.28 ± 18.4	2.60 ± 6.37	−1.0 ± 10.51	NR	NR
8	25.4 ± 20.5	−2.9 ± 5.81	−17.8 ± 27.3	−1.95 ± 6.92	−9.63 ± 15.36
9	NR	NR	6.7 ± 25.8	−1.74 ± 7.41	6.0 ± 21.2
Mean	−5.36	−2.30	−0.87	−1.92	−0.67
SD	22.05	5.23	17.50	5.40	14.65

NR = No Result, DS = Designed system, SPH = Sphygmocor system

Table C.2: Comparison of time variation of the systolic peak.

No.	RMS Error (mmHg) (Mean ± S.D.)				
	Method 1		Method 2		Method 3
	DS	SPH	DS	SPH	DS
1	10.7± 2.77	3.9 ± 1.47	12.1 ± 4.5	3.9 ± 1.9	13.3 ± 4.44
3	5.37± 1.73	1.06± 0.48	4.07± 1.97	1.43 ± 0.72	11.72 ± 2.61
4	4.25 ± 1.84	2.26± 1.05	4.61± 0.62	2.76 ± 1.76	10.33 ± 1.64
5	4.08 ± 1.15	1.36 ± 0.65	3.02 ± 1.31	NR	NR
6	4.74 ± 3.41	1.81 ± 0.47	3.40 ± 1.10	2.18 ± 0.56	4.95 ± 1.86
7	6.85 ± 1.85	2.38 ± 0.37	6.67 ± 4.36	2.69 ± 0.42	35.83 ± 5.95
8	18.73 ± 9.17	10.20 ± 6.55	45.55 ± 42.21	12.65 ± 7.9	28.8 ± 9.43
9	NR	NR	12.82 ± 6.90	2.50 ± 1.15	14.75 ± 7.75
Mean	7.50	3.11	11.35	3.80	18.01
SD	6.02	3.60	18.9	4.41	15.98

NR = No Result, DS = Designed system, SPH = Sphygmocor system

Table C.3: Comparison of RMS error between individual pulses.

C.3 Results of Time Analysis

The designed system and the Sphygmocor system were compared by analysising the differences in the systolic peak, the dicrotic notch and the second systolic peak. The results of these comparisons are presented in Tables C.4 – C.11.

Table C.4 and Table C.5 compare the systolic blood pressure error for the designed system and the Sphygmocor system respectively. The error is the difference between the mean blood pressure as calculated by the calibration algorithm and the blood pressure measured with cuff sphygmomanometer.

No.	Measured SBP (mmHg)	Mean SBP (mmHg)	Error (mmHg)	% Error (%)
1	130	132.9 ± 7.8	2.94 ±7.88	2.26 ± 6.07
3	134	134.7 ± 2.7	0.74 ± 2.7	0.55 ± 2.0
4	130	130.6 ± 3.1	0.6 ± 3.1	0.45 ± 2.4
5	120	120.3 ± 3.4	0.3 ± 3.4	0.25 ± 2.86
6	118	118.2 ± 3.3	0.2 ± 3.3	0.001 ± 0.03
7	124	124.8 ± 8.3	0.9 ± 8.3	0.7 ± 6.7
8	250	262.5 ± 58.2	12.5 ± 58.2	5.0 ± 23.3
9	114	115.8 ± 6.6	1.8 ± 6.6	1.6 ± 5.7
Mean	140	139.9	2.3	1.3
SD	44.9	47.6	18.9	8.3

Table C.4: Comparison of systolic pressure measured from designed system

No.	Measured SBP (mmHg)	Mean SBP (mmHg)	Error (mmHg)	% Error (%)
1	130	130.1 ± 6.18	−0.15 ±6.18	−0.11 ± 4.75
3	134	134.1 ± 1.8	0.11 ± 1.8	0.08 ± 1.34
4	130	129.9 ± 4.7	0.03 ± 4.7	0.02 ± 3.62
5	120	120.1 ± 1.9	0.06 ± 1.9	0.05 ± 1.60
6	118	118.0 ± 3.7	0.02 ± 3.7	0.00 ± 0.03
7	124	125.9 ± 1.5	1.89 ± 1.5	1.52 ± 1.19
8	250	250.3 ± 19.2	0.32 ± 19.2	0.13 ± 7.68
9	114	113.9 ± 3.5	−0.02 ± 3.5	−0.02 ± 3.06
Mean	140	138.9	0.10	0.07
SD	44.9	41.6	6.67	3.36

Table C.5: Comparison of systolic pressure measured from sphygmocor system

Table C.6 compares the systolic rise time between the two systems. The error is calculated from the mean of the pulse for each subject.

No.	DS (ms)	SPH (ms)	Error (ms)	% Error (%)
1	92	96	−4.0	−4.2
3	75	84	−9.0	−10.7
4	78	95	−17.0	17.9
5	112	104	8.0	7.7
6	85	86	−1.0	−1.2
7	78	81	−3.0	−3.7
8	105	103	2.0	1.9
9	96	97	−1.0	−1.0
Mean	90.1	92	−1.9	−2.4
SD	13.6	9.1	5.3	5.6

DS = Designed system, SPH = Sphygmocor system

Table C.6: Comparison of rise time of the systolic peak

Table C.7 and C.8 compare the pressure and timing of the dicrotic notch between the two systems for each subject.

No.	DS (ms)	SPH (ms)	Error (ms)	% Error (%)
1	274	285	−11.0	−3.9
3	246	252	−6.0	−2.4
4	267	285	−18.0	−17.9
5	288	296	−8.0	−2.7
6	306	299	7.0	2.3
7	308	306	2.0	0.7
8	278	288	−10.0	−3.5
9	350	324	26.0	8.0
Mean	289.6	291.88	−2.3	−2.4
SD	31.7	20.7	13.8	7.4

DS = Designed system, SPH = Sphygmocor system

Table C.7: Comparison of time to the dicrotic notch

Table C.9 and C.10 compare the pressure and timing of the second systolic peak between the two systems for each subject.

No.	DS (mmHg)	SPH (mmHg)	Error (mmHg)	% Error (%)
1	101	93	8.0	8.6
3	96	99	−3.0	−3.0
4	90	98	−8.0	−8.2
5	85	86	−1.0	−1.2
6	90	95	−5.0	−5.3
7	96	100	−4.0	−4.0
8	137	122	15.0	12.3
9	84	95	−11.0	−11.6
Mean	97.4	98.5	−1.1	−1.6
SD	17.0	10.5	8.57	8.1

DS = Designed system, SPH = Sphygmocor system

Table C.8: Comparison of dicrotic notch value

No.	DS (mmHg)	SPH (mmHg)	Error (mmHg)	% Error (%)
1	101	97	4.0	4.1
3	104	103	1.0	0.9
4	105	108	−3.0	−2.8
5	88	89	−1.0	−1.1
6	93	97	−4.0	−4.1
7	99	102	−3.0	−2.9
8	153	155	−2.0	−1.3
9	85	96	−11.0	−11.5
Mean	103.5	105.9	−2.3	−2.3
SD	21.3	20.6	4.4	4.5

DS = Designed system, SPH = Sphygmocor system

Table C.9: Comparison of second systolic peak

No.	DS (ms)	SPH (ms)	Error (ms)	% Error (%)
1	296	356	−60.0	−16.9
3	312	321	−9.0	−2.8
4	373	397	−24.0	−6.0
5	451	393	58.0	14.8
6	373	371	2.0	0.5
7	352	376	−24.0	−6.4
8	359	390	−31.0	−7.9
9	376	353	23.0	6.5
Mean	361.5	369.6	−8.1	−2.3
SD	46.8	25.6	36.2	9.7

DS = Designed system, SPH = Sphygmocor system

Table C.10: Comparison of time to second systolic peak

Table C.11 presents the RMS Error between the designed system and th Sphygmocor system. The error is calculated from the average pulse for each subject.

No.	RMS Error (mmHg)
1	5.55
3	6.16
4	9.54
5	13.50
6	5.04
7	8.34
8	22.77
9	9.08
Mean	9.99
SD	5.83

Table C.11: Comparison of Root-Mean-Square (RMS) errors

C.4 Frequency Spectrum Results

The frequency spectrum for subjects 1–9 are illustrated in Figures C.9–C.16. Figures C.9–C.16 (a) present the spectrum for the designed system, Figures C.9–C.16 (b) present the spectrum for the Sphygmocor system and Figures C.9–C.16 (c) compares the spectrum of the two systems.

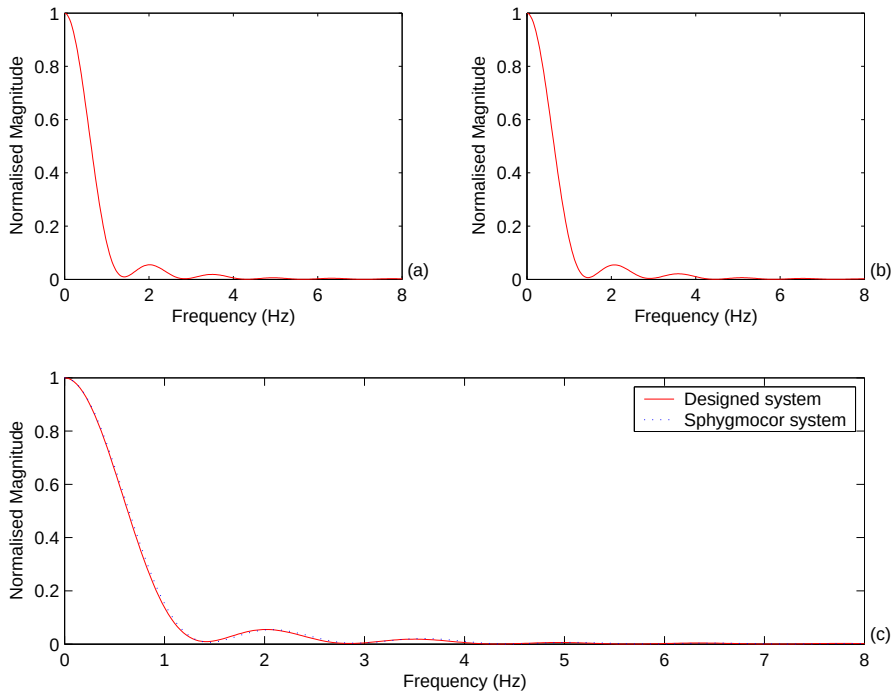


Figure C.9: Frequency spectrum of subject 1: (a) Frequency spectrum of the designed system; (b) Frequency spectrum of the Sphygmocor system; (c) Comparison of the frequency spectrum between two systems

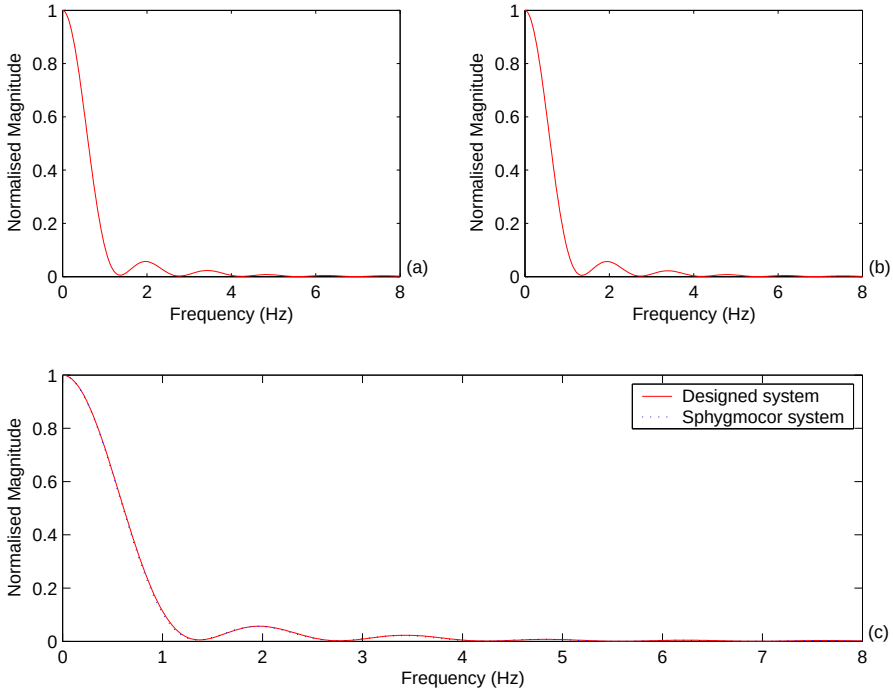


Figure C.10: Frequency spectrum of subject 3: (a) Frequency spectrum of the designed system; (b) Frequency spectrum of the Sphygmocor system; (c) Comparison of the frequency spectrum between two systems

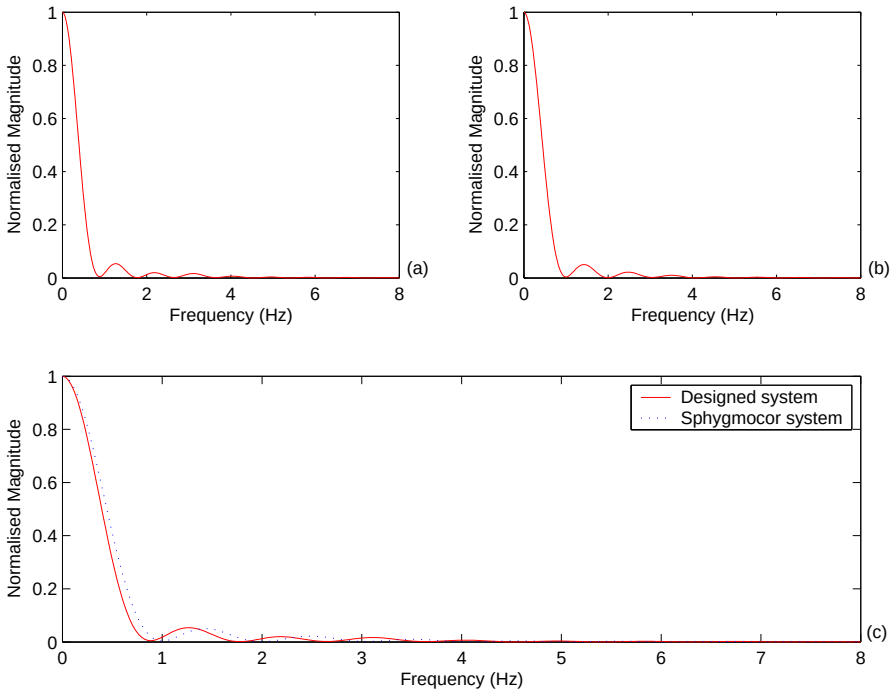


Figure C.11: Frequency spectrum of subject 4: (a) Frequency spectrum of the designed system; (b) Frequency spectrum of the Sphygmocor system; (c) Comparison of the frequency spectrum between two systems

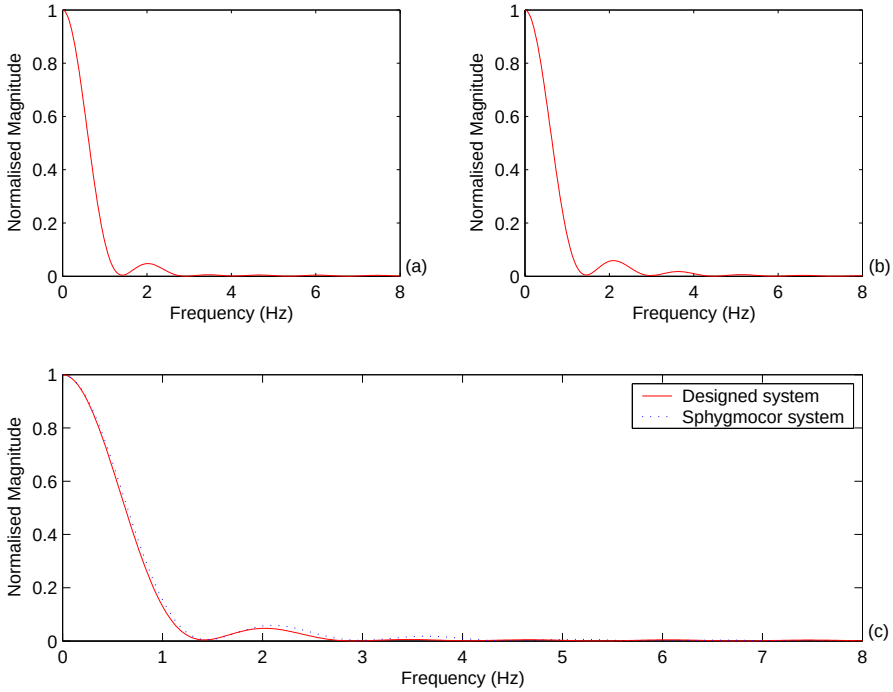


Figure C.12: Frequency spectrum of subject 5: (a) Frequency spectrum of the designed system; (b) Frequency spectrum of the Sphygmocor system; (c) Comparison of the frequency spectrum between two systems

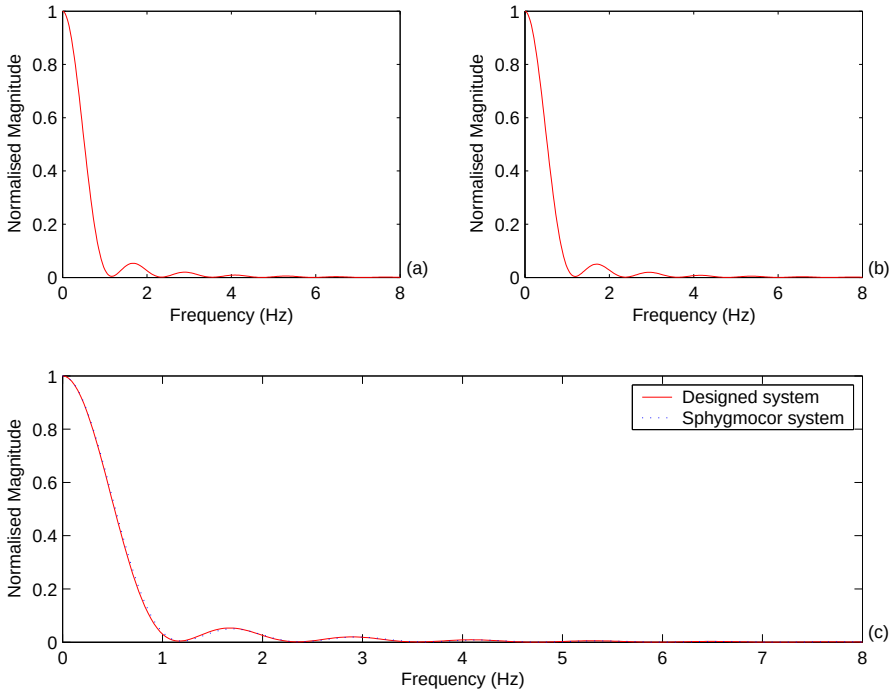


Figure C.13: Frequency spectrum of subject 6: (a) Frequency spectrum of the designed system; (b) Frequency spectrum of the Sphygmocor system; (c) Comparison of the frequency spectrum between two systems

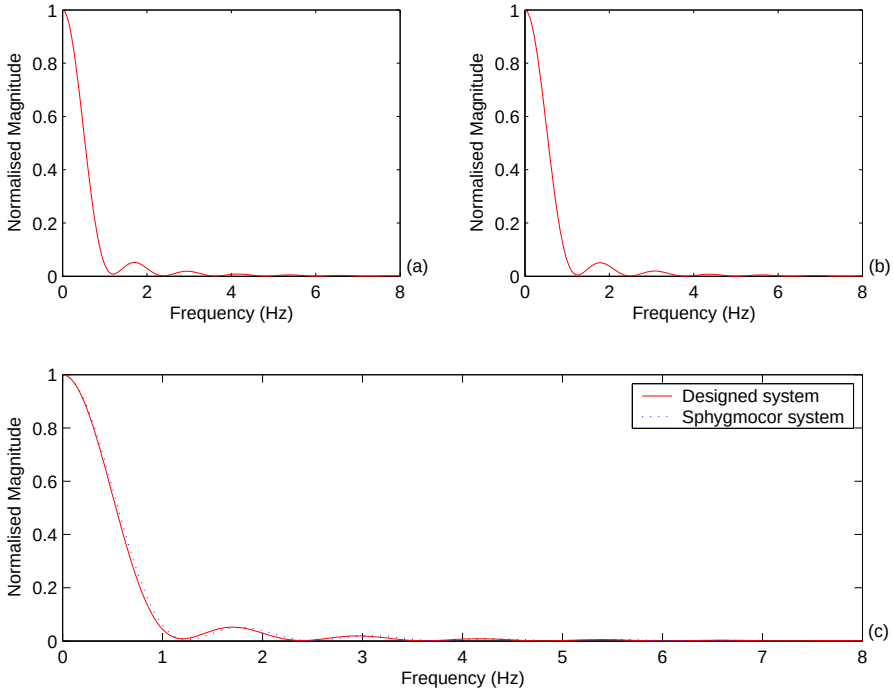


Figure C.14: Frequency spectrum of subject 7: (a) Frequency spectrum of the designed system; (b) Frequency spectrum of the Sphygmocor system; (c) Comparison of the frequency spectrum between two systems

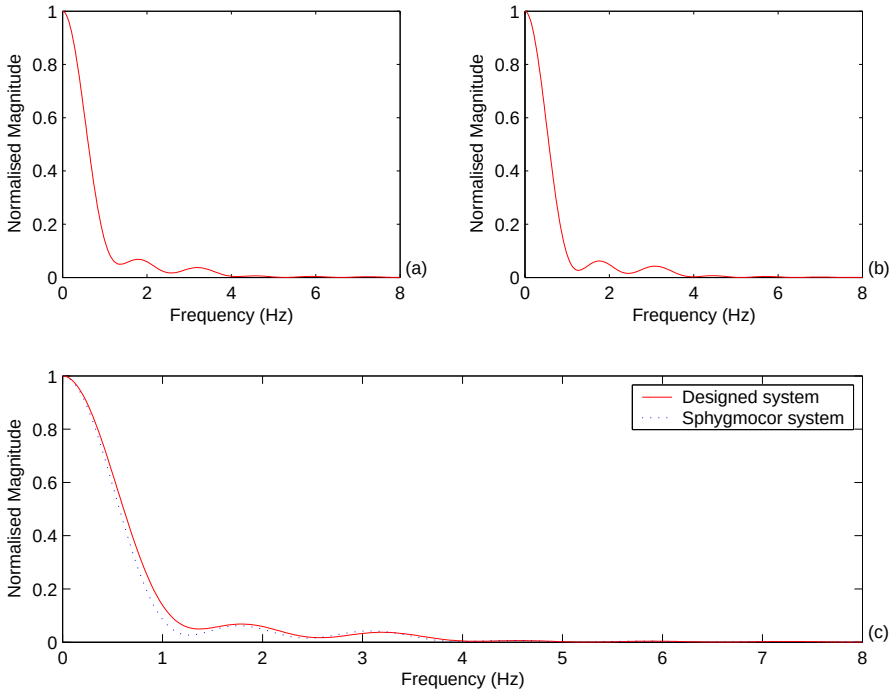


Figure C.15: Frequency spectrum of subject 8: (a) Frequency spectrum of the designed system; (b) Frequency spectrum of the Sphygmocor system; (c) Comparison of the frequency spectrum between two systems

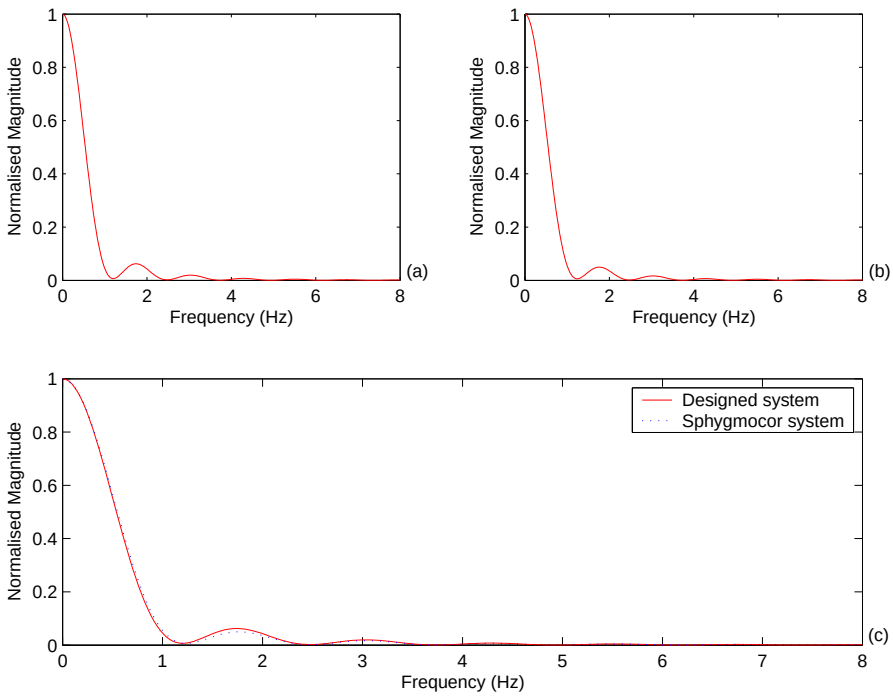


Figure C.16: Frequency spectrum of subject 9: (a) Frequency spectrum of the designed system; (b) Frequency spectrum of the Sphygmocor system; (c) Comparison of the frequency spectrum between two systems

Appendix D

IEC Test Results

The printouts of the IEC 601-1 tests are included below.

Appendix E

Ethics Approval

The clearance certificate from the human research ethics committee is attached to this appendix.

References

[1] O'Rourke, M.F., Pauca, A., Jiang, X., "Pulse wave analysis," *Research methods in human cardiovascular pharmacology*, vol. 51, pp. 507–522, 2001.

[2] Karamanoglu, M. and Feneley, M. P., "On-line synthesis of the human ascending aortic pressure pulse from the finger pulse," *Hypertension*, vol. 30, pp. 1416–1424, 1997.

[3] van Lieshout, J.J., Toska, K., van Lieshout, E.J., Eriksen, M., Walloe, L., Wesseling, K.H., "Beat-to-beat noninvasive stroke volume from arterial pressure and doppler ultrasound," *European Journal of Applied Physiology*, vol. 90, pp. 131–137, 2003.

[4] Oliver, J.J. and Webb, D.J., "Noninvasive assessment of arterial stiffness and risk of atherosclerotic events," *Arteriosclerosis, Thrombosis, and Vascular Biology*, vol. 23, pp. 554–566, 2003.

[5] Brinton, T.J., Cotter, B., Kailasam, M.T., Brown, D.L., Chio, S., O'Conner, D.T., DeMaria, A.N., "Development and validation of a noninvasive method to determine arterial pressure and vascular compliance," *The American Journal of Cardiology*, vol. 80, pp. 323–330, 1997.

[6] Cruickshank, K., Rista, L., Anderson, S.G., Wright, J.S., Dunn, G., Gosling, R.G., "Aortic pulse-wave velocity and it's relationship to mortality

in diabetes and glocose intolerance." *Circulation*, vol. 106, no. 16, p. 2085, 2002.

[7] Hlimonenko, I., Meigas, K., Vahisalu, R., "Waveform analysis of peripheral pulse wave detected in the fingertip with photoplthysmograph," *Measurement Science Review*, vol. 3, pp. 49–52, 2003.

[8] Wilkinson, I.B., Fuchs,S.A., Jansen, I.M., Spratt, J.C., Murray, G.D., Cockcroft, J.R. and Webb, D.J., "Reproducibilty of pulse wave velocity and augmentation index measured by pulse wave analysis," *Journal of Hypertension*, vol. 16, pp. 2079–2084, 1998.

[9] Weber, T., Auer, J., O'Rouke, M., Kvas, E., Lassig, E., Berent, R., Eber, B., "Arterial stiffness, wave reflections, and the risk of coronary artery disease," *Circulation*, vol. 109, pp. 184–189, 2004.

[10] Millasseau,S.C., Patel,S.J., Redwood,S.R., Ritter,J.M., Chowienczyk,P.J., "Pressure wave reflection assessed from the peripheral pulse: Is a transfer function necessary?" *Hypertension*, vol. 41, pp. 1016–1020, 2003.

[11] Savage, M.T., Ferro, C.J., Pinder, S.J., Tomson, C.R.V., "Reproducibility of derived central arterial waveforms in patients with chronic renal failure," *Clinical Science*, vol. 103, pp. 59–65, 2002.

[12] Wilkinson, I.B., Hall, I.R., MacCullum, H., Mackenzie, I.S., McEniery, C.M., van der Arend, B.J., Shu, Y., Mackay, L.S., Webb, D.J., Cockcroft, J.R., "Pulse Wave Analysis: Clinical evaluation of a noninvasive, widely applicable method for assessing endothelial function," *Arteriosclerosis, Thrombosis, and Vascular Biology*, vol. 22, pp. 147–152, 2002.

[13] Segers, P., Carlier, S., Pasquet, A., Rabben, S.I., Hellevik, L.R., Remme, E., de Backer, T., de Sutter, J., Thomas, J.D., Verdonck, P., "Individualizing the aorto-radial pressure transfer function: feasibility of a model based approach," *American Journal of Physiology - Heart and Ciculartory Physiology*, vol. 279, pp. H542–H549, 2000.

[14] McLeod, A.L., Uren, N.G., Wilkinson, I.B., Webb, D.J., Maxwell, S.R.J., Northridge, D.B., Newby, D.E., "Non-invasive measures of pulse wave velocity correlate with coronary arterial plaque in humans," *Journal of Hypertension*, vol. 22, no. 2, pp. 363–368, 2004.

[15] Lemogoum, D., Flores, G., Van den Abeele, W., Ciarka, A., Leeman, M., Degaute, J. P., van de Borne, P., Van Bortel, L., "Validity of pulse pressure and augmentation index as surrogate measures of arterial stiffness during beta-adrenergic stimulation," *Journal of Hypertension*, vol. 22, no. 3, pp. 511–517, 2004.

[16] Asmar, R., Benetos, A., Topouchian, J., Laurent, P., Pannier, B., Brisac, A., Target, R., Levy, B.I., "Assessment of arterial distensibility by automatic pulse wave velocity measurement," *Hypertension*, vol. 26, no. 3, pp. 485–490, 1995.

[17] Steiner, L.A., Johnston, A.J., Salvador,R., Crozsnyka, M., Menon, D.K., "Validation of a tonomertric noninvasive arterial blood pressure monitor in the intensive care setting," *Anaesthesia*, vol. 58, pp. 448–454, 2003.

[18] The South African Bureau of Standards, "SABS IEC 60601-1, Medical electrical equipment, Part 1: General requirements for safety," The South African Bureau of Standards, Tech. Rep., 1988.

[19] O'Rourke, M.F. and Gallagher, D.E., "Pulse wave analysis," *Journal of Hypertension*, vol. 14 (suppl 5), pp. S147–S157, 1996.

[20] Meyer, B.J. Meij, H.S. Meyer, A.C., *HUMAN PHYSIOLOGY*, 2nd ed. Juta & Co, Ltd, 1997.

[21] Izzo, J.l. and Shykoff, B.E., "Arterial stiffness: Clinical relevance, measurement, and treatment," *Reviews in Cardiovascular Medicine*, vol. 2, no. 1, pp. 29–40, 2001.

[22] Bronzino,J.D., *THE BIOMEDICAL ENGINEERING HANDBOOK*, 2nd ed. CRC Press, 2000, vol. 1.

[23] Davies,J.I. and Struthers, A.D., "Pulse wave analysis and pulse wave velocity: a critical review of their strengths and weaknesses," *Journal of Hypertension*, vol. 21, pp. 463–472, 2003.

[24] O'Rourke, M.F., Avolio, A., Qasem, A., "Clinical assessment of wave reflection," *Hypertension*, vol. 42, no. 5, pp. e15–e16, Nov 2003.

[25] Salter, G.D., Bird, E., "Evaluation of arterial stiffness by measurement of pulse wave velocity (PWV)," University of the Witwatersrand, Johannesburg, Tech. Rep., October 2002, Project report.

[26] McLaughlin, J., McMeill, M., Braun, B., McCormack, P.D., "Piezoelectric sensor determination of arterial pulse wave velocity," *Physiological Measurement*, vol. 24, pp. 693–702, 2003.

[27] van Brakel, A., Swart, P.L., Chtcherbakov, A.A., Shlyagin, M.G., "Blood pressure manometer using a twin Bragg grating Fabry-Perot interferometer," *Photonics Asia, Beijing, China, 8-12 Nov 2004, Proceedings of SPIE*, vol. 5634, no. 86, November 2004.

[28] ICSensors, "Data Sheet model 84," April 2000.

[29] Analog Devices, "AD620 Low cost, Low power, instrumentation amplifier," Analog Devices,Inc.," Data Sheet, 1999.

[30] Texas Instruments, "Information for medical applications," Texas Instruments," Application note, 2004.

[31] Stapletin, H. and O'Grady, A., "Isolation techniques for high-resolution data-acquisition systems," *EDN Magazine (www.ednmag.com)*, pp. 113–118, February 2004.

[32] Hewlett Packard, "High CMR Isolation Amplifer," Hewlett Packard," Data sheet.

[33] Fairchild semiconductor, "General purpose 6-pin phototransistor optocouplers," Fairchild Semiconductor Corporation," Data sheet, 2003.

[34] J. Bentley, *PRINCIPLES OF MEASUREMENT SYSTEMS*, 3rd ed. Pearson Education Limited, 1995.

[35] Chiu, Y.C., Arand, P.W., Schroff, S.G., Feldman, T., Carroll, J.D., "Determination of pulse wave velocities with computerised algorithms," *American Heart Journal*, vol. 121, no. 5, pp. 1460–1469, 1991.

[36] Fetics, B., Nevo, E., Chen, C., Hass, D.A., "Parametric model derivation of transfer function for noninvasive estimation of aortic pressure by radial tonometry," *IEEE Transactions on Biomedical Engineering*, vol. 46, no. 6, pp. 698–706, 1999.

[37] Cooper, G.R., McGillem, C.D., *PROBABILISTIC METHODS OF SIGNAL AND SYSTEM ANALYSIS*, 1st ed. Oxford University Press, 1999.

[38] Bruce, E.N., *BIOMEDICAL SIGNAL PROCESSING AND SIGNAL MODELLING*, 1st ed. John Wiley and Sons, Inc., 2001.

[39] IC Sensors, Markell ,K., "A simple pressure sensor signal conditioning circuit," August 1999, Application note.

[40] Analog Devices, "AD623 Single supply, rail-to-rail, low cost instrumentation amplifier," Analog Devices,Inc.," Data Sheet, 1999.

[41] Horowitz, P. and Hill, W., *THE ART OF ELECTRONICS*, 2nd ed. Cambridge University Press, 1989.